Contents lists available at ScienceDirect

Structural Safety

journal homepage: www.elsevier.com/locate/strusafe

Performance evaluation of high-rise buildings using database-assisted design approach

Dikshant Saini, Bahareh Dokhaei, Behrouz Shafei, Alice Alipour *

Iowa State University, United States

ARTICLE INFO

Keywords:
Performance based design
Tall buildings
Time domain
Wind pressure
Database-assisted design (DAD)

ABSTRACT

In recent years, performance-based design (PBD) has gained attention and is sought to be the benchmark approach in the field of wind engineering. While the concept of performance-based design is well-accepted in earthquake engineering, it is yet to be embraced for the design of buildings to resist severe wind loads. This paper introduces a framework for the performance-based wind design (PBWD) of tall steel buildings using a time domain analysis that keeps the process of wind effects and the structural design process integrated, transparent, and fully auditable. From the perspective of PBWD, the main objective is to achieve a desirable performance level for a given hazard level, i.e., mean recurrence interval of extreme wind. The wind effects are directly related to the mean annual return of wind through a well-accepted simulation approach. A 180 m tall standard CAARC building is used for the case study to illustrate the proposed methodology. The wind load time histories are determined using the pressure tap data on exterior faces of the building measured in the wind tunnel. With the calculated wind loads, nonlinear dynamic analysis is conducted with various wind directions and mean wind speeds based on database-assisted design (DAD) approach. The key performance measures such as demand-to-capacity indices, inter-story drift, damage deformation index, and floor accelerations are calculated as a function of wind directions and mean wind speed. The obtained responses are used in conjunction with a local wind climatological database to determine the extreme wind effects for any specific mean recurrence interval. The performance of the steel building is evaluated for three performance criteria, including occupant comfort, operational, and continuous occupancy. The conducted performance assessment reveals that building fails to satisfy the serviceability requirement of drifts. However, the building satisfies the requirements for the occupant comfort and operational performance levels for strength design, while it also satisfies the continuous occupancy, limited interruption in Risk category II. The result reveals that the proposed framework provides realistic assessment of performance of the building incorporating the wind directionality and return period of the wind speeds.

1. Introduction

Performance-based design (PBD) approach describes a process to economically design the structures to meet certain performance criteria as specified by owners and stakeholders. The main objective of PBD is to give flexibility to the owner allowing them to tailor their design based on the importance of the structure, location, and economic constraints. In wind engineering, a PBD approach will provide an opportunity to design structural systems with development of controlled nonlinearity in structural members, which is not allowed in the existing design codes. The target performance levels for critical structures may be kept strict, while more lenient performance levels can be used for structures that may not be as vital while in operation. With lenient performance levels, some damage may be allowed to occur but not so much that the structure would collapse. As a result, the structure would be taken out of operation or retrofitted after a major event. With the urban development and planning policies, the number of tall buildings is increasing in urban areas. In several cities such as New York, Orlando and Houston, these buildings are often subjected to extreme wind loads arising from hurricanes. In recent studies focusing on the impact of climate change [1–3], it is identified that the frequency and intensity of the high intensity storms are set to increase in future. Many researchers worked on decreasing the intensity on wind-induced hazards [4–8]. This increasing extreme wind weather will result in increased demands on the main

* Corresponding author.
E-mail address: alipour@iastate.edu (A. Alipour).

https://doi.org/10.1016/j.strusafe.2024.102447
Received 15 November 2021; Received in revised form 8 January 2024; Accepted 27 January 2024

wind force resisting systems. Therefore, a reliable approach is needed to assess the performance of the tall buildings beyond the design loads [9]. The current design code specifies equivalent static design loads for the design of structural members. The current strength-based approach does not address the serviceability design criteria of the buildings under normal or extreme wind loads. In addition, the existing design approach does not allow inelasticity in the structural members therefore making the structure and the owners vulnerable to potential damages due to higher than design wind loads, which are becoming more likely. Therefore, a PBD approach is needed, which may address the shortcomings of the existing prescriptive design code.

In the past decade, the PBD approach has become a topic of interest in the wind engineering community for the design of buildings. In response to the increasing interest, ASCE has published the first edition of the pre-standard for the performance-based wind design [10]. This is primarily intended to distinguish between the performance objectives of the wind design and seismic design. It is believed that the PBD can still take several years to become mainstream design method for the practitioners. Several studies have focused on developing a framework for the PBD of buildings subjected to wind loads [11–15]. Several studies have focused on the PBD of buildings against wind loads using nonlinear time history analysis [16–21]. In one of the early studies, Solari [15] and Solari and Piccardo [22] investigated the wind excited response of structures based on Taylor series expansions incorporating uncertainties of model parameters and modeling errors. It was observed that first order expansions provided accurate solutions with subsequent increase in accuracy with second order expansions. Muthukumar et al. [21] conducted a performance assessment of an existing building by considering inelastic behavior of various parts of the building. Based on the performance evaluations, the building owner was able make decisions to retrofit the building. In a separate effort, Hart and Jain [16] proposed a procedure for performance assessment and strengthening of existing buildings subjected to wind loads. Judd and Charney [17] investigated nonlinear behavior of the building using wind load measured in wind tunnel testing. Incremental dynamic analysis (IDA) is performed to calculate the risk of collapse by incorporating the epistemic uncertainties. In another study, Mohammadi et al. [20] investigated the performance of an existing high-rise building by performing incremental dynamic analysis. The performance of the building is evaluated using story drift ratios and floor acceleration levels as a function of basic wind speeds. Although the analysis considered the nonlinear response of the beams and columns, the wind directionality effects are not considered. More recently, Ghaffary and Moustafa [23] conducted performance assessment of a 20-story SAC building under wind loads at different wind speeds. Nonlinear dynamic analysis of the two-dimensional building model was performed in OpenSEES. In their study, a two-dimensional model was developed which could not be used to analyze along-wind and across-wind response of the building simultaneously. Chuang and Spence [24] noted that the main challenge in probabilistic PBWD was the computational cost of conducting nonlinear time history analyses for tall buildings exposed to long-duration wind storms, however, they developed an effective method to evaluate the inelastic response of structures under wind loads. In a series of studies, Ouyang and Spence [24] investigated the PBD approaches for multi-story buildings under wind loads considering damage mechanism from excessive pressures and damages from multiple hazards and assessed the performance of building envelopes in wind-excited engineered systems. Ouyang and Spence [25] integrated the PBD approach in a stochastic simulation framework including the probabilistic models for extreme directional speed and concurrent rainfall hazard, pressure field models, wind driven rain models, damage models and loss models. Although the proposed framework is comprehensive enough to estimate the system level loss and its consequences, a simplified model is used for considering the wind directionality. Such simplifications can possibly cause missing the worst-case scenarios for the structural members.

Hareendran and Alipour [26] has recently studied the nonlinear response of tall buildings when exposed to wind loads that vary randomly over a prolonged period of 30 min. In their study, a 44-story steel frame building is analyzed using PBD, considering different wind speeds and evaluating structural responses such as acceleration, displacement time histories, and member forces. The study also involved the examination of fragility curves as a useful approach to optimize the design of nonstructural elements in wind-sensitive high-rise buildings, and evaluate damage states and repair costs [27]. The studies, however, did not consider the influence of varying wind directions. For performance-based wind design (PBWD), time-history wind loads are determined via wind tunnel tests. However, Jeong et al. [28] investigated the generation of time-history wind loads from power spectral density (PSD) functions for inelastic examination, including vertical distribution and maximum oriented load happening. Huang and Chen [29] conducted a numerical investigation of tall building responses to simultaneous independent along wind and crosswind loads. They explored the impact of the P-Delta effect and material yield stress on the time history and statistical moment of the inelastic building responses in comparison to elastic responses. They also showed that the yielding caused a non-Gaussian crosswind response with kurtosis less than 3 and a lower peak factor compared to traditional elastic response, which follows a Gaussian distribution [30]. This study emphasized the importance of considering simultaneous actions of both wind loads and provided valuable insights for the performance-based design of tall buildings in extreme wind conditions [29]. In another study, Huang and Chen [31] focused on assessing the precision of a simplified model to analyze inelastic responses in tall buildings subjected to both alongwind and crosswind loads. This simplified model is built using modal push-over analysis and represents the building's inelastic response through its fundamental modes in primary directions. It was found that the mean wind load leads to inelastic displacement drift, and the fluctuating component can be estimated separately. While the study offers valuable insights, it does not address the complexities and challenges associated with applying the model to buildings with 3D coupled mode shapes.

Abdelwahab et al. [32] provide a comprehensive overview of PBWD specifically tailored for tall buildings. The paper focuses on differentiating PBWD from Performance-Based Seismic Design (PBSD) and sheds light on the challenges associated with implementing PBWD. It highlights the importance of studying the nonlinear inelastic response of structures when subjected to wind loads and evaluates the performance of building envelopes in windy conditions [33]. It can be seen that several studies have investigated the performance of building under wind loads but the performance of the building is determined as a function of wind speed for a few dominant wind directions at a local site. Furthermore, the adopted building models are mostly elastic, not providing an understanding of the post-elastic response of the considered buildings or are two-dimensional and preventing the consideration of the along- and across-wind, and torsional responses and their interaction in the performance estimation of the building. This leads to the approaches used in the past research for the wind performance assessment of buildings to not cover the worst-case scenarios for all the structural members. Additionally, the return period of wind speeds in different storm types can vary significantly between wind directions. Therefore, a limited number of wind directions may not provide the extreme wind effect in all the members. These issues can be properly addressed with the use an approach that can efficiently use the wind climate models to reflect this variability [34–36]. Using such an approach the most realistic estimation of wind loads is used for the PBD of buildings under wind loads. Since the framework is based on direct simulations, the structural response obtained is directly related to the mean annual return of wind.

To address the highlighted gaps, this study proposes a PBWD framework that uses the simulation techniques based on DAD approach. The main objective is to define the performance level in terms of mean recurrence intervals (MRI) while the structural response is determined in the form of response surfaces by conducting nonlinear time history

analysis considering the along- and cross-wind and torsional responses. As an illustration of the proposed framework, a case study of 45-story steel tall building is presented. For the detailed performance evaluation, the considered engineering demand parameters include floor acceleration levels, inter-story drift ratios, demand-to-capacity indices (DCIs) and deformation damage index (DDI). In this study, three performance levels and their acceptance criteria are defined. The response surfaces are used to determine the requisite wind effects for specific mean recurrence intervals using the local climatological database. The case study results indicate that the proposed framework can be used for the PBWD of tall buildings. This study consists of five sections. Section 2 provides a detailed description of the PBWD framework along with performance objectives and evaluation criteria. This is followed by Section 3, which provides the details of the 45-story steel building and its modeling details considering post-elastic response as well as the details of the model validation. Section 4 presents the response of the building using the PBWD approach described in Section 2. Section 5 provides the important conclusions and possible areas of future work.

2. Framework for performance based wind design

PBD is a widely accepted approach in earthquake engineering. However, there is still a lack of consensus about the procedure for designing buildings against wind loads, which can capture the different damage states of the buildings. A typical process of PBD consists of three components i.e., hazard analysis, response analysis, and loss analysis. The most organized document for the hazard analysis is the recently published Prestandard for Performance Based Wind Design [10], which prescribes three methods of linear or nonlinear time history analysis for PBWD. In the first method, the building response is determined from the linear time history analysis. If the demand to capacity values observed are high (as defined in the pre-standard), the designer will need to perform a detailed nonlinear history analysis. The second and third methods directly evaluate the structural reliability with the target reliabilities as defined in ASCE 7–16 [37]. The pre-standard also specifies minimum performance objectives for three performance levels of occupant comfort, operational, and continuous occupancy with limited interruption. From the overview of performance levels, it can be observed that only limited inelasticity of structural members is permitted for the wind loads in contrast to the significant nonlinear behavior considered for the seismic loads. This is because significant yielding of structural members can reduce frequencies of vibration of structure under the seismic loads. The reduced frequencies will reduce the demand on most structures. However, this reduction in frequencies can result in an increased wind load effect, which may result in an underestimation of the design. Another aspect is the general expectation of the society, which expects the buildings to remain elastic under winds.

For the performance evaluation of the buildings, three performance levels are considered, i.e., occupant comfort, operational, and continued occupancy with limited interruption. The first performance level of occupant comfort is defined as independent of the risk category, while different MRIs are specified for operational and continuous occupancy with limited interruption performance objectives. For the occupant comfort, the structural system is intended to remain elastic with building motions and vibrations minimizing the occupant discomfort at design wind of 1 month, 1 year and 10-year MRI. At this performance level, the acceptance criteria are defined as frequency dependent peak acceleration limits. Fig. 1 shows the 10-year MRI peak acceleration values for office and residential buildings as a function of fundamental frequency of the building. The peak acceleration values for the residential buildings are 2/3 of the values established for office buildings. In addition to acceleration values in Fig. 1, the acceleration values suggested by Chang [38] are also used. Table 3 presents the peak acceleration levels ranging from 5 mg to 150 mg for five comfort limits. The second objective is defined as the operational limit state at which the structural system should also remain elastic. At this performance level, a peak drift ratio of

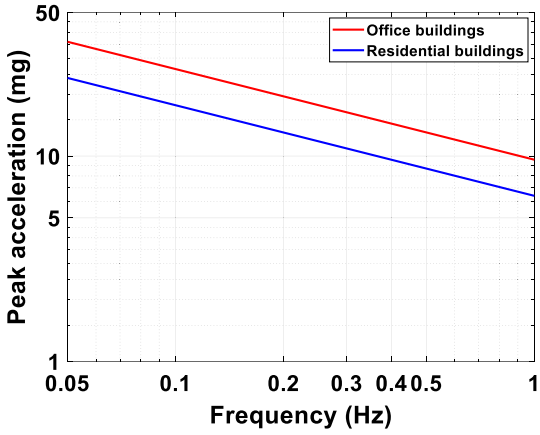

Fig. 1. Frequency dependent acceleration limits for occupant comfort for 10 year MRI [39].

H/400 with no residual drift ratio is assumed. For the third performance objective of continuous occupancy, limited plastic behavior is allowed in some specific elements or components that recommended by Mohammadi et al. [20]. The structural system is required to withstand the wind loads with low probability of partial or total collapse. A value of H/200 is assumed for the peak drift ratio. In addition to the deformation-based limits, strength limits are defined on the force controlled (e.g., shear wall) and deformation-controlled elements (e.g., beams and columns). The strength limits to identify the performance level of the structural members are adopted from a previous study by Mohammadi et al. [20]. According to their study, for the limit state corresponding to occupant comfort, the DCI index is assumed to be 0.5. The structure is assumed to be in linear elastic phase where the forces in the structural members do not exceed 50 % of the design strength. In case of operational limit state, the DCI index limit is taken as 1.0 i.e., all the structural members are still in the elastic range. On the other hand, the DCI index should not exceed 1.25 for the elements with deformation-controlled resistance for the continuous occupancy limit state. In this state, non-linearity in the response of structural members is allowed but limited to overstressing of 25 % beyond available design strength. In the case of force-controlled elements, the DCI index is limited to 1.0.

From the perspective of PBWD approach, the ultimate objective is to determine the performance of the structure for a given MRI of wind hazard. Therefore, it is important to determine wind speeds and wind directionality for assessing wind loads and structural response at varying return periods. For identifying wind speeds and wind directionality, two approaches i.e., ASCE 7–16 [37] codified values and site-specific wind climate analysis, are available. The first approach results in more conservative values compared to site-specific analysis. This is because ASCE 7–16 [37] codified values consider the largest force coefficient and largest non-directional wind speed for design. Although the site-specific climate analysis is more appropriate, accurate estimation of wind directionality effects remains a challenge. These issues can be resolved with the use of DAD approach.

The DAD approach provides a realistic estimation of wind load distributions and incorporates wind directionality effects. DAD has several advantages over the traditional methods such as ASCE 7–16 [37] for the design of buildings against the extreme wind loads as it can capture the across wind as well as the aero-elastic effects in tall buildings. In addition, it is inherently superior to other methods in capturing the wind directionality effects. The method is based on the significant advancement made to the use of pressure gauges for estimating the aerodynamic wind loads on tall buildings and employs the full set of aerodynamic pressure data for the design of structures under wind loads. This includes the measurement of time series data of pressure coefficients at several locations on building models tested in the wind tunnel, and data of

directional wind speeds measured at the building site [40–43]. In this study, a database assisted PBWD approach is proposed for tall buildings under wind loads. The outline of the proposed framework is shown in Fig. 2. The process of estimating performance of the structural system can be decomposed into two components: (1) Structural response evaluation, and (2) wind directionality effects.

2.1. Structural response evaluation

The structural response of the building can be obtained by performing time history analysis of the building. For that purpose, aerodynamic loads can be obtained by either conducting wind tunnel tests or computational fluid dynamics simulation. Wind tunnel tests are generally conducted to determine pressure time data at various locations using pressure gauges, and this measured data is subsequently employed to calculate the aerodynamic loads on the structure. This method is considered more accurate as compared to static analysis method specified by design codes. Structural response evaluation aims at determining the structural response of the system for combinations of wind speeds and wind directions. For the sets of wind speeds and wind directions, the performance of building is evaluated by determining the wind effects of structures such as internal forces of the structural members, acceleration and drift response of building, and the base shear and overturning moments. While acceleration and drift response are used to check the serviceability design, DCIs are used to evaluate the strength design. For the strength design, the performance of the structure is assessed by calculating the demand to capacity ratios of the entire structural member, which is defined by DCIs. The DCIs for the structural members such as beams, and columns are calculated using the following equations from AISC 360–16 [44]:

$$DCI = \frac{P_r}{\varnothing_p P_n} + \frac{8}{9}\left(\frac{M_{rx}}{\varnothing_m M_{nx}} + \frac{M_{ry}}{\varnothing_m M_{ny}}\right) if \frac{P_r}{\varnothing_p P_n} \geq 0.2 \quad (1)$$

$$DCI = \frac{P_r}{2\varnothing_p P_n} + \left(\frac{M_{rx}}{\varnothing_m M_{nx}} + \frac{M_{ry}}{\varnothing_m M_{ny}}\right) if \frac{P_r}{\varnothing_p P_n} < 0.2 \quad (2)$$

where P_r and P_n are the required and available axial strength; M_r and M_n are the required and available flexural strength; $\varnothing_p$ and $\varnothing_m$ are the resistance factors, which is assumed to be 0.9 based on load and resistance factor design (LRFD) method.

In this study, another performance criterion that is related to the cladding system's performance due to significant inter-story shear strain deformations is assessed. Instead of drift ratios, the DDI is evaluated as suggested by Griffis [45]. The DDI can analyze the shear strain in an element by detecting the displacement at four nodes of an element. The DDI of the ABCD sheet, as shown in Fig. 16(a), can be determined analytically using Equation (3). Fig. 16(a) illustrates the method that can be used to calculate DDIs of cladding components. This is due to the fact drift limits cannot always capture the damage caused by the shear deformation.

$$DDI = 0.5\left[\frac{X_A - X_C}{H} + \frac{X_B - X_D}{H} + \frac{Y_D - Y_C}{L} + \frac{Y_B - Y_A}{L}\right] \quad (3)$$

In this study, the building is assumed to have metal claddings. To assess the performance of such cladding systems, DDI values of 1/100, 1/75, and 1/50 are used for occupant comfort, operational, and continuous occupancy with limited interruption performance levels [10].

This information can be used to develop response surfaces i.e., plots of structural response measures as a function of wind speeds and wind directions. These response surfaces are developed for peak value of DCIs, DDIs, inter-story drift ratios, and accelerations. It should be noted that the ordinates of the response surfaces are not proportional to the square of the wind speeds owing to interaction of along and across-wind, torsional effects, and inherent nonlinearities associated with the response of structure. Therefore, dynamic time history analysis should be conducted to account for dependency of engineering demand parameters on wind directions and wind speeds.

2.2. Wind directionality

The developed response surfaces depend on the aerodynamic and structural properties of the structure, which are independent of the local wind climate. For applying the wind directionality effects, the structural responses with specified MRIs are determined by considering the dependence of both wind speeds and structural response upon direction. For evaluating the performance of the structural system, it is important to calculate the peak wind effects for the given MRI. The peak wind effects are obtained by using the wind climatological database and the developed response surfaces. A typical wind climatological database may consist of record of 1000s of extreme wind events consisting of wind velocities and wind directions. The peak wind effects are obtained

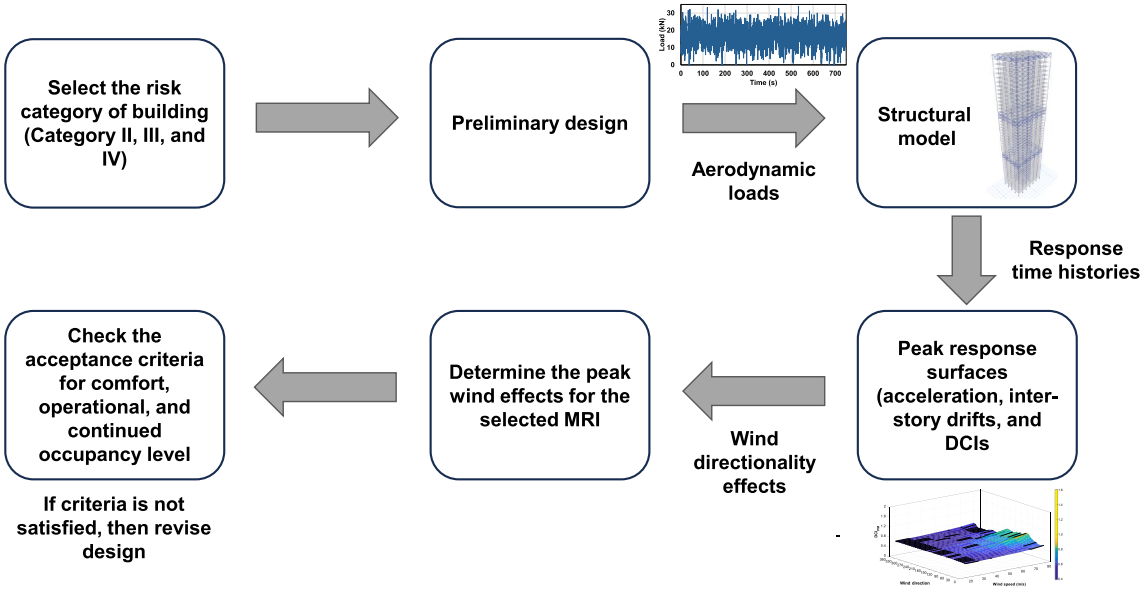

Fig. 2. Proposed framework for integration of database -assisted design and performance-based design of tall buildings.

Table 1
Performance objectives for the buildings under wind loads (ASCE-PBWD 2019 [10]).

Risk category	Continuous occupancy, limited interruption (LI)	Operational (OP)	Occupant comfort (OC)
II	700-year MRI	10-year MRI	Risk category independent
III	1700-year MRI	25-year MRI	
IV	3000-year MRI	50-year MRI	

by transforming the wind speed matrix ($[U_{rs}]$) into matrix of peak wind effects $[(R^{pk}(U_{rs})]$. This process will provide the components of wind effects consisting of largest values in each of n windstorms. However, the maximum of these wind effects are the quantities, which captures the extreme response of the structure. In the next steps, $[(R^{pk}(U_{rs})]$ is transformed into a vector $[(R^{pk}(U_r)]^T$, where T denotes the transpose of the matrix. This is done by ignoring R in each row lower than $R^{pk}(U_r)$. Lastly, non-parametric statistic is used in conjunction with mean annual rate of storm arrival (λ) to obtain the quantities $R^{pk}(\bar{N})$. The MRI of the i^{th} highest-ranking value R^{pk} can be obtained using the following equation:

$$\bar{N}_i = \left[1 - \exp(-\frac{\lambda k}{n+1})\right]^{-1} \tag{4}$$

where n represents the number of storms. It is noted that the peak of wind effect may not always correspond to maximum wind speed. The detailed process for obtaining the directional wind effects is explained in [46]. There is potential to consider more directions and use the correlation of wind speed and direction for more accuracy. However, this is out-of-scope of the current manuscript, the intent of which is to provide a procedure for performance-based wind design considering nonlinearity and with use of database-assisted design approach. If the intention is to provide a detailed directionality analysis in the context of PBWD, one can use the techniques introduced by Carta et al. [47], where a joint distribution model incorporating wind speed direction marginal distributions is proposed. Exploring this area further could be valuable for investigating the effects of wind directionality.

By accounting for the wind directionality, the DCIs, DDIs, inter-story drift ratio, and acceleration values are calculated with the specified design MRI, which are directly checked with the acceptance criteria of the desired performance objectives as specified in Table 1 and Table 2. If the design does not meet the performance criteria, the structural members are then resized to achieve the desired performance level at a specified MRI.

3. Case study 45-story steel building

This section illustrates the integrated PBWD approach using a case study with a tall steel building. The nonlinear dynamic analysis of the building is performed using OpenSEES [48] for 10 wind directions and 15 wind speeds. For each analysis, key response measures such as the DCIs, DDIs, peak inter-story drift ratio, and peak acceleration are obtained. A detailed description of the building design, modeling details, and response of the building are provided in the following subsections.

3.1. Description of the structure

The case study building is a 45-story standard moment resisting frame CAARC (Commonwealth Advisory Aeronautical Council) building. The building has a height (H) of 182.88 m, width (b) of 45.72 m, and depth (d) of 30.48 m i.e., b/d ratio is 1.5. The building consists of two types of columns i.e., core, and perimeter columns. Fig. 3 shows the schematic views of the 45-story steel building. The dimensions of each type of columns are kept same for 15 successive floors. All the beams consist of a rolled W-sections from AISC 360–16 [44] whereas the columns are made up of built-up hollow structural sections (HSS). The

Table 2
Performance levels and their acceptance criteria (ASCE-PBWD 2019 [10]).

Performance levels	Response measures		
	Acceleration	Story drift	Residual story drift
Occupant comfort	Yes (1 month, 1 year, and 10 year)	–	–
Operational	–	H/400	–
Continuous occupancy, limited interruption	–	H/200	H/1000

Table 3
Acceleration limits for serviceability performance criteria of occupant comfort [38].

Peak floor acceleration (mg)	Comfort limit
<5	Not perceptible
5–15	Threshold of perceptibility
15–50	Mild discomfort
50–150	Severe discomfort
> 150	Intolerable

building is assumed to have a 175 mm thick floor slab at all floor levels. Due to the floor slab, a full composite action is expected between the floor beams and floor slab. In addition to the self-weight, a live load and super-imposed dead load of 2.4 kN/m^2 and 0.72 kN/m^2 is applied at each floor, which are typical loads, expected for the office building. A detailed description of the section properties is given in Table 4. All the structural members are assumed to be of Grade 50 steel with a yield stress of 345 MPa. Wind directions are defined in clockwise direction with X-axis parallel to the short dimension of the building. The building is assumed to have an orientation of 270° from the north. The building is assumed to be in Newark, New Jersey (Milepost 2500) with suburban terrain on all sides. The structural system is designed based on weak beam and strong column theory. The demand to capacity ratio of the structural members does not exceed 1 for a design mean wind speed of 105.0 mph (46.9 m/s).

3.2. Analytical model

To analyze the performance of the building, a three-dimensional nonlinear model is developed using a finite element software OpenSEES [48]. In the chosen building, the interior as well as the exterior building columns are assumed contributing to the lateral resistance of the building. The building model is developed using a combination of elastic beam column elements and nonlinear spring elements. The nonlinearity of the beams, columns, panel zones, and connections is modeled using the nonlinear spring elements. Rigid diaphragm behavior provided by the floor slab is captured using the nodal constraints at the floor level. The moment of area of the floor beams is doubled to capture the full composite action between the floor beams and floor slab.

The nonlinear behavior of beams and columns is modeled using a combination of elastic beam column elements and two zero-length spring elements. These two zero-length spring elements are assumed to capture the concentrated nonlinearity in the beams and columns. The plastic hinges for the columns are considered at top and bottom of the column, while the beams are assumed to form plastic hinges at a distance of half the beam's depth from the column face. The cyclic behavior of the plastic hinges is modeled using the modified Ibarra-Krawinkler (MIK) model [49]. This model simulates the nonlinear moment–curvature relationship of beams and columns using a multilinear monotonic backbone. For modeling the column panel zones at the beam column joints, the parallelogram model proposed by Gupta and Krawinkler [50] is adopted. This model consists of an assembly of rigid elements and nonlinear spring elements to capture the yielding and

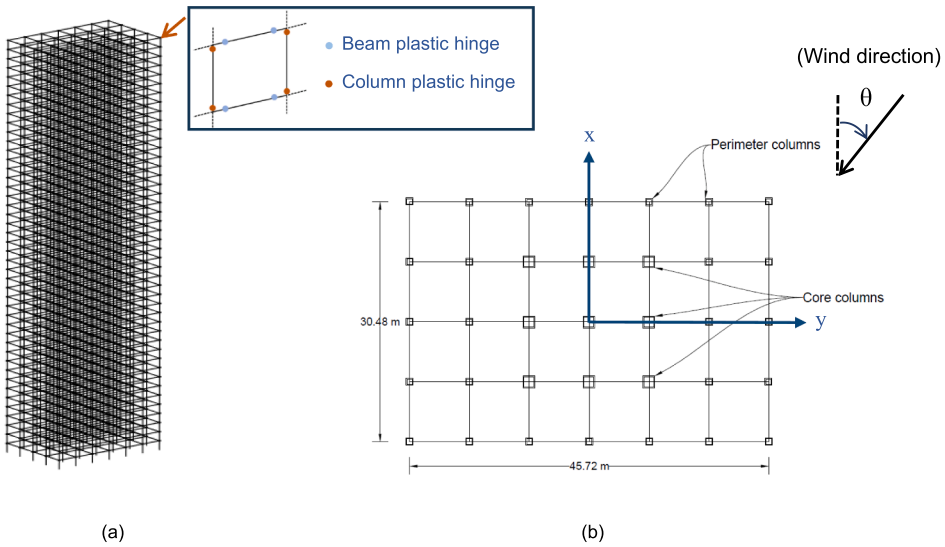

Fig. 3. 45-story steel building model: (a) isometric view of the building including the schematics of the plastic hinges, and (b) plan view of the building and the angle of attack of the buildings.

Table 4
Section properties for the structural members in the 45-story building.

Member type	Section type	Depth (mm)	Width (mm)	Flange thickness (mm)	Web thickness (mm)
Core columns	HSS	1371.6	1371.6	101.6	101.6
	HSS	1066.8	1066.8	76.2	76.2
	HSS	914.4	914.4	50.1	50.1
Perimeter columns	HSS	1066.8	1066.8	76.2	76.2
	HSS	1066.8	1066.8	50.8	50.8
	HSS	914.4	914.4	38.1	38.1
Beam	I/Wide Flange	254.0	254.0	14.2	8.6

post-yield behavior of panel zones. Fig. 4 shows the three-dimensional representation of the panel zone model along with the hinges in beams and columns.

3.3. Dynamic time history analysis using aerodynamic loads

In this study, the wind tunnel data is obtained from a database available at NIST (www.nist.gov/wind). The test data is obtained from wind tunnel tests on a rigid model. Therefore, the aeroelastic effects are assumed not to be present. The wind tunnel test was performed for wind directions between 0° and 360° using a reduced scale model with a length scale of 1:500. For each wind direction, the data in terms of pressure coefficients (C_p) was collected for 30 s at a mean hourly wind speed (V_H) of 23.2 m/s (suburban terrain exposure) at the rooftop elevation (H) of the building model. The measured pressure coefficients are assumed to be independent of the Reynolds number. This assumption leads to the fact that the measured pressure coefficients will be identical for the model and the prototype. The aerodynamic data consisted of 30 pressure taps on each face of building model i.e., a total of 120 pressure taps. The pressure taps were placed in a rectangular pattern on each face of building model. However, the wind tunnel testing may not consist of enough number of pressures tap to calculate the floor loads directly. Fig. 5 illustrates the procedure used to calculate the floor loads in the study following the work by Park and Yeo [34]. In the first step, the virtual pressure taps are created at the edge of the model surface. The pressure time data at those locations is obtained by extrapolating the data using the pressure taps at the outermost and next to outermost locations. The entire domain is then discretized in small grids considering the pressure tap at the center of each grid. The pressure time data at the center of mesh grid is obtained by performing cubic interpolation in MATLAB. From the obtained pressure distribution, the wind loads are calculated by multiplying the pressure time data and the corresponding tributary area. In the computational model, the wind loads are applied at the beam column joints, as shown in Fig. 5. This combination of loads will ultimately capture the X-direction, Y-direction, and torsional direction wind loads acting on the building. It should be noted that the pressure data obtained from the wind tunnel laboratory is measured at reduced scale. Therefore, the wind loads obtained using the pressure data are scaled up using appropriate length scale and time scale. The magnitude of the wind loads calculated from the wind tunnel laboratory is scaled up using the square of velocity scale (V_p/V_m) and time scale. Time scale is used to modify the sampling time in the prototype loading, which is defined as follows:

$$\Delta t_p = \frac{L_p V_m}{L_m V_p} \Delta t_m \tag{5}$$

where (L_p/L_m) is the length scale, and Δt_m is the time step of data in the model. This shows that the time step in the prototype depends on the wind speed under consideration.

A nonlinear time history analysis is performed for a set of wind speeds and a set of wind directions. The analysis is performed for a range of wind velocities between 25.0 m/s and 60.0 m/s (with an interval of 2.5 m/s). The reference height for the mean hourly wind speed is assumed to be the height of the building. For each wind velocity, a total number of 10 wind directions between 0° and 90° are considered. Overall, a total of 150 nonlinear time history analyses are performed which provides comprehensive data to evaluate the dynamic response of the building. This step is important to calculate the wind effects for a particular MRI with the inclusion of wind directionality effects. For the chosen building, the dynamic analysis is conducted with a total of 552 time-history nodal loads around the building. This scheme of wind load application comprehensively captures the spatial variation along the height as well as the width of the building. Each analysis was conducted for a total duration of 30 min with a 10 sec added ramp in the beginning of all loading histories. In this study, the use of a single loading time history record for each calculation at various wind directions has disregarded the potential variations in wind loading and response among different records. This limitation arises from two main factors. Firstly, the reliance on wind tunnel test data from NIST's database for wind data instead of employing stochastically generated time histories. Secondly,

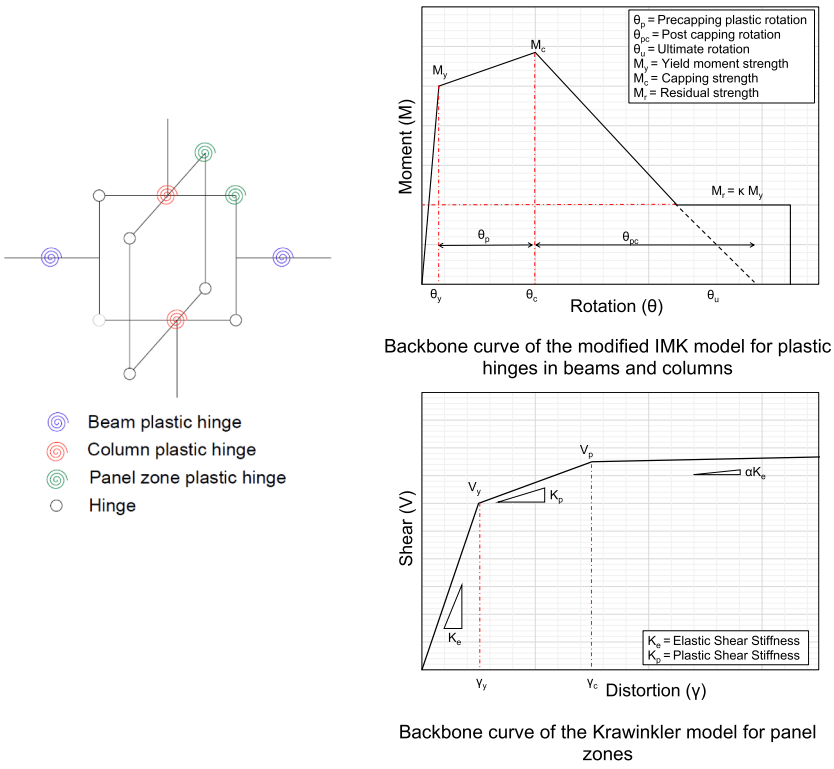

Fig. 4. Modeling details to capture the non-linear behavior of moment resisting frames of building under wind loads.

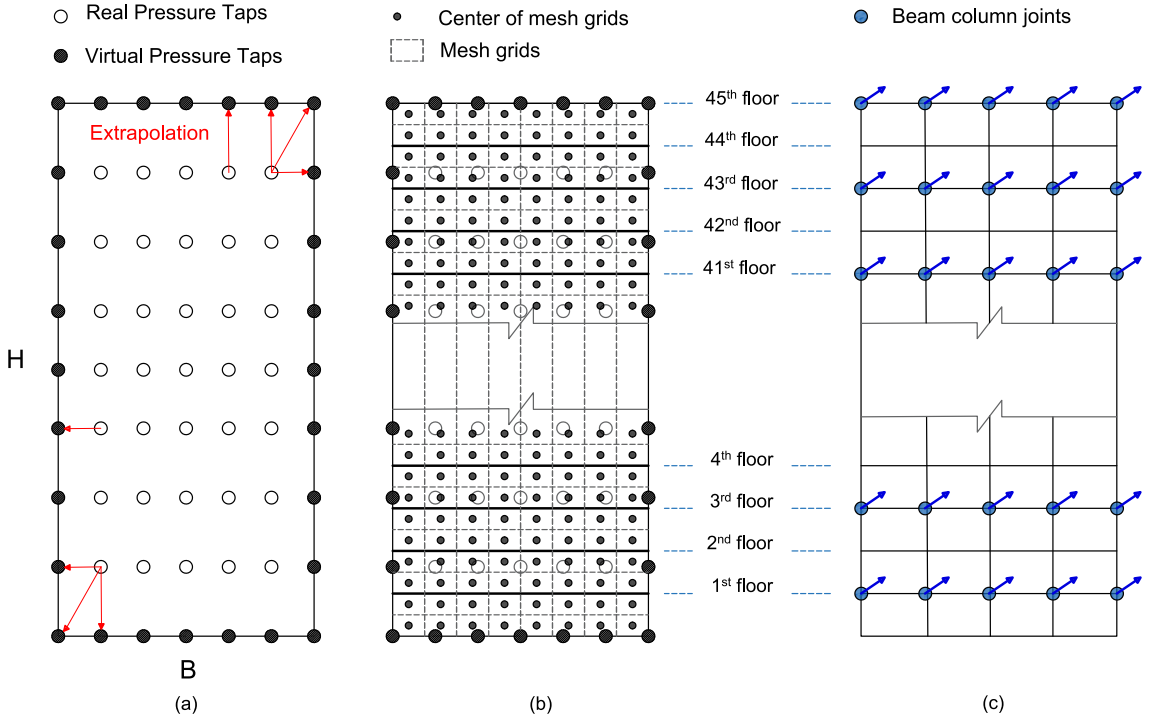

Fig. 5. Schematic representation of the procedure to calculate the wind forces applied at the floor level: (a) extrapolating pressures at edges, (b) interpolating pressures in mesh grids, and (c) applying loads normal to the surface.

the utilization of the DAD methodology in PBWD has restricted the examination of response variability among different records.

The peak DCIs, DDIs, inter-story drift ratios, and accelerations are obtained from their time histories induced by the effective wind loads combined with gravity loads such as dead loads and live loads. The following load combination as specified in the ASCE 7–16 is used:

$$L = 1.2\ DL + 1.0\ LL + 1.0\ WL \tag{6}$$

Where *DL*, *LL*, and *WL* represent dead load, live load, and wind load, respectively. The second order effects i.e., p-delta effects, are considered

in the time history analysis. This is important as the secondary effects are found to have significant influence on drift ratio as well as demand to capacity ratio of the structural members.

3.4. Model validation via seismic analysis

For validation of the modeling procedure, the current study replicates the response of two by one four-story moment resisting frame building. This building was tested to collapse at the E-Defense shake table facility in September 2007 [51,52]. It is crucial to acknowledge that there is limited availability of experimental data for larger steel buildings, which prompted the decision to concentrate on a structure of this size. While the chosen building model may not directly match the scale of larger steel buildings, it successfully generated numerical models that effectively capture the nonlinear response of structures. The building had plan dimensions of 6 m × 10 m along the X- and Y-directions as shown in Fig. 6. The first story height was 3.875 m, while rest of the stories had a height of 3.5 m. In the tested building, the columns were made up of HSS sections with outer dimensions of 300 mm and wall thickness of 9 mm. The building consisted of wide flange beams with structural depth ranging from 300 mm to 400 mm. At the floor level, a 175 mm thick concrete slab was placed due to which a full composite section was expected. The building was tested under progressively increased ground motion intensities of the JR Takatori motion (1995 Kobe earthquake). The building was tested to 20 %, 40 %, 60 %, and 100 % of the original JR Takatori record. The east–west (EW) component of the ground motion was assigned to the Y-direction, while the north–south (NS) component of the ground motion was given as input in the X-direction. For each of the ground motion intensity, the response of the building was evaluated in terms of inter-story drift ratios, base shear, and deformed shapes.

Prior to the dynamic simulations, the mode shapes and time period of the four-story building are obtained. The time period corresponding to first two modes are found 0.82 and 0.76 in comparison to 0.80 and 0.76 observed during the experiments. The dynamic simulations are performed for ground motion intensities of 20 %, 40 %, 60 %, and 100 %. Fig. 7 shows the comparison of the peak inter-story drift ratios obtained from simulations and experiments. The difference in the drift values can

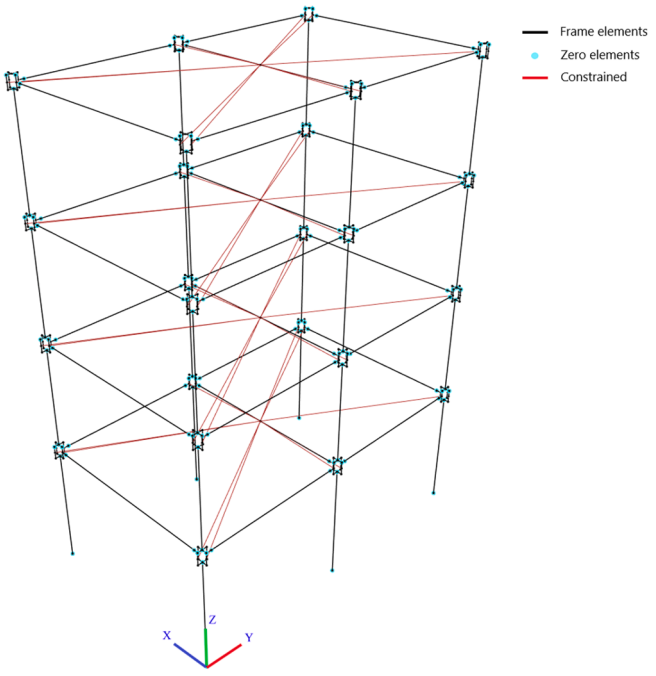

Fig. 6. Schematic of the validation model in OpenSees from E-Defense shake table of 4-Story building.

be attributed to two reasons. The first reason is the difference in the uncertainties in the model parameters capturing the elastic plastic behavior. The second reason is the modeling of the mass of structure. Unlike the distributed mass of structural and non-structural components in the experiments, the mass is lumped at the beam column joints in the simulations. Further, the response of the building is also compared for the ground motion intensity of 100 %. During the experiments, the building is observed to collapse with significant plastic hinge formation in the first story columns. Fig. 8 clearly shows the simulations can accurately predict the time as well the base shear of the building during the collapse. From the model validation study, it is concluded that the modeling strategy can be adopted to capture the nonlinear response of the building under dynamic loads such as wind loads.

4. Results and discussions

Prior to the main simulations, the modal analysis of the building with the initial dimensions of the members is conducted. Fig. 9 presents the mode shapes and time periods for the first six modes of the building. As expected, the first two modes of the building are along the major axis of the building. The third mode of the building is observed to be torsional. From the time periods, the building is observed to be relatively flexible indicating building will undergo large displacements under lateral loads. Following up with the modal analysis, the investigation focuses on the time-history dynamic analysis of building under wind loads. From the comprehensive dynamic analysis, the response surfaces including acceleration, inter-story drift ratio, and DCIs are obtained for each wind velocity and wind direction.

4.1. Structural response

The structural response for load combination in Equation 6 is evaluated by calculating the acceleration values at each floor, inter-story drift ratio as well as DCI and DDI indices for structural members. The acceleration, DDI, and the inter-story drift ratio values govern the serviceability design of the building, while DCI values govern the strength design of buildings. For each analysis, the acceleration and inter-story drift values are calculated at the center of each floor of the building in X-and Y-directions. For both linear and nonlinear responses of the building, the floor accelerations are observed to be maximum at the roof level. During the linear response, the peak inter-story drift ratio occurs in 15th and 16th story of the building, while the location of the peak inter-story drift changes to 44th and 45th story during the nonlinear response of the building. Fig. 10 and Fig. 11 present the floor acceleration, and floor displacement time histories at several floors of the building for wind direction of 90°. In general, floor accelerations and displacements increase along the height of the building. The acceleration responses indicate that, for wind direction of 90°, the maximum acceleration in the X-direction surpasses that in the Y-direction. This discrepancy in vibration can be attributed to two potential factors: building stiffness and wind loading. There are two possible reasons for this observed difference in vibration: building stiffness, and wind loading. Examining the fundamental modal periods for both translational directions, which are 8.88 s and 8.55 s, respectively, reveals no significant difference in stiffness. Therefore, the difference in the response is not predominantly due to the difference in stiffness. Instead, the dissimilarity in responses between both directions can be attributed to variations in wind loads. A key factor contributing to greater vibrations in X-direction (perpendicular to the wind direction in this case) compared to Y-direction (parallel to the wind direction in this case) is known as vortex shedding. Vortex shedding occurs when wind flows around the building, creating an unbalanced pressure distribution on the cross-sectional area. This phenomenon leads to increased vibrations in the across-wind direction. The acceleration plot demonstrates that the applied wind loads effectively capture both along-wind and across-wind responses of the building. Consequently, the increased response in the

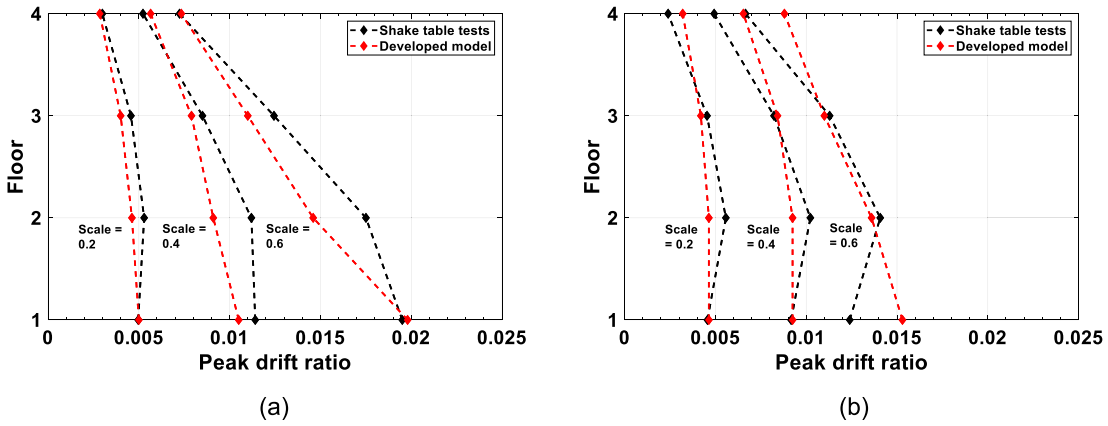

Fig. 7. Comparison of peak story drift ratios obtained from experiments and simulations of a four-story moment resisting frame: (a) X loading direction, and (b) Y loading direction.

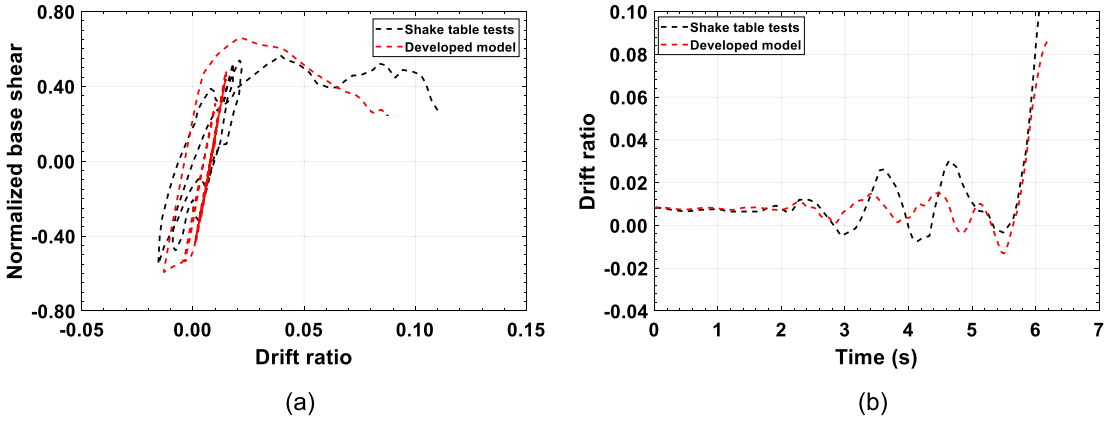

Fig. 8. Model validation results for the four-story moment resisting frame: (a) normalized base shear versus drift ratio, and (b) drift ratio versus time.

direction perpendicular to the wind depends on the influence of cross-wind pressure.

To further study the time-varying displacement response of the top floor, Fig. 12 illustrates the time history of top floor displacements in the X-direction and Y-direction at a wind angle of 0° for wind speeds of 40 and 60 m/s. This figure shows both linear and nonlinear responses, which correspond to high wind speeds. The wind-induced displacement responses comprise two components: fluctuating displacement and time-varying mean displacement. The mean displacement in the along-wind direction is considerably more pronounced than the nearly negligible mean displacements in the across-wind direction, as there is no static wind load in the crosswind direction. However fluctuating component is more significant in across wind direction displacements. Notably, the Y-direction exhibits a fluctuating response with a zero-mean due to vortex shedding from the wind flow across the wind direction, and this fluctuation intensifies with increasing wind speed. The time history of X-direction displacement has both time-varying mean and fluctuating components. For wind speed of 40 m/s, the time-varying mean component of X-direction displacement initially increases and then reaches to a low steady state value which is determined by the mean wind load. However, with a wind speed of 60 m/s, the time-varying mean component shows a higher value and increases over time, ultimately resulting in damage to the building structure, significantly elevating the time-varying mean displacements. Moreover, the fluctuating component in Y-direction displacement was much greater than X-direction fluctuating displacement.

In this study, one loading time history analysis was conducted for each wind direction and speed, utilizing wind tunnel test data instead of numerically generated wind loading time histories. However, it's worth noting that Ding and Chen [53] demonstrated that the extreme response distribution could be predicted from a single response, relying on statistical moments of the response [29,30]. To visualize the response distribution, Fig. 13 presents the mean, standard deviation (STD), kurtosis, and peak factor of X-direction displacement for the top floor, under wind speeds of 30, 40, 50, and 60 m/s, and wind directions of 0°, 30°, 60°, and 90° for a duration of 150 s. The peak factor represents the ratio of maximum response to the standard deviation of response, while kurtosis offers insights into the tails' characteristics of the probability distribution, effectively describing its shape of distribution. When kurtosis equals 3, the distribution exhibits similar tail behavior to a normal distribution. In Fig. 13(a), it is evident that an increase in wind velocity corresponds to a rise in the mean X-direction displacement. Additionally, changing the wind direction from 0° to 90° leads to a decrease in the mean X-direction displacement, primarily because 0° and 30° directions align closely with the static wind load. Fig. 13(b) demonstrates that higher wind velocities and changing the wind directions from 0° to 90° result in an increased standard deviation of X-direction displacement. This is due to the higher fluctuations in response at 90°, where the wind direction is perpendicular. Fig. 13(c) reveals that the kurtosis of displacement response falls between 1.9 and 3.6. For wind directions of 0°, 30°, and 60°, the kurtosis remains below 3, which is the kurtosis of normal distribution, while for a wind direction of 90°, the kurtosis surpasses the kurtosis of a normal distribution. Finally, in Fig. 13(d), the peak factor for displacement is observed to range between 1.7 and 2.7.

The focus of the current study has been on examining these extreme responses. An extreme response refers to the maximum or peak level of

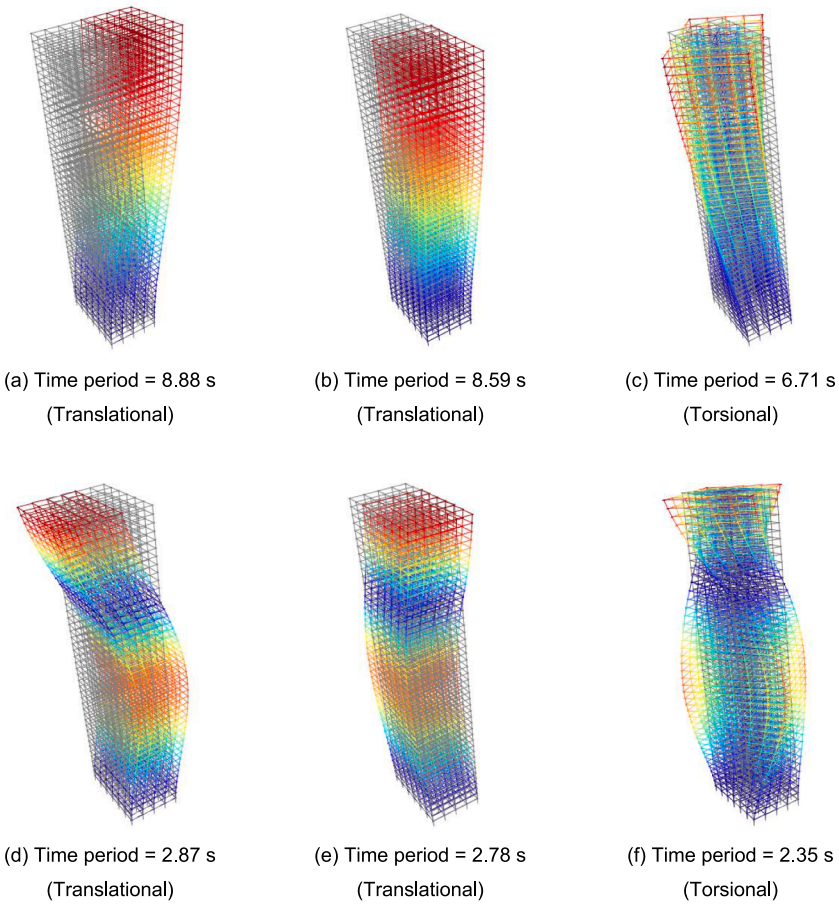

Fig. 9. Elastic response, fundamental period and mode shapes of the building.

response that the structure experiences as a result of wind loads. By quantifying the maximum response, the performance of the building can be evaluated, and compliance with serviceability requirements can be assessed.

4.1.1. Floor accelerations

Fig. 14 shows the plot for peak floor accelerations measured at the center and corner of floor as a function of wind speeds and wind directions. The peak floor acceleration values at the center of floor in both X- and Y- direction are calculated and shown in Fig. 14(a) and 14(b), respectively. For considering the effect of torsion in acceleration, the peak floor acceleration values at the corner of the floor are calculated separately for the X- and Y- directions, shown in Fig. 14(c) and 14(d), respectively. Along with the acceleration values, the performance criteria related to motion comfort are also plotted which are adopted from [38]. Significantly higher peak floor acceleration values are observed in the X-direction, primarily because of the influence of wind-induced vortex shedding, which exerts a more pronounced effect on the building's larger dimension, thereby leading to a more pronounced response in the X-direction. The lower periods indicate that the building is flexible which translates into significantly larger floor accelerations of the building. At low wind speeds, torsion in floor acceleration has an insignificant effect on the performance level. The highest values for peak floor acceleration in the X-direction and Y-direction occur at wind directions of 90° and 0°, respectively. Torsional effects were considered by analyzing the maximum acceleration at the corner location of the model, as these locations are more susceptible to torsional forces. Due to the torsion occurring in different wind directions, the corner accelerations were found to increase by 12 % and 25 % in the X-direction and Y-direction respectively.

Without considering torsion, from the acceleration values in X-direction, the motion comfort can be in the mild discomfort range even at a wind speed of 25.0 m/s for the wind direction of 80° and 90°. When the wind speed is increased to 37.5 m/s, the floor accelerations can be very discomforting for the occupants for the wind directions of 80° and 90°. With further increase in wind speed above 45.0 m/s, wind loads from most the wind directions are observed to cause accelerations that can be very discomforting. On the other hand, the accelerations in the Y-direction are only observed to be in the range of severe discomfort for the wind direction of 0° and 10°. For wind speeds greater than 55.0 m/s, the floor accelerations can become intolerable to the occupants which happens when the building collapses or is about to collapse. This is further explained using the inter-story drift values.

Considering torsion, the motion comfort in the X-direction follows a similar pattern, with mild discomfort at a wind speed of 25.0 m/s for wind directions of 80° and 90°. As the wind speed increases to 37.5 m/s, the floor accelerations become very discomforting for occupants at wind directions of 80° and 90°. With further increase in wind speed above 42.5 m/s, wind loads from most wind directions cause accelerations that can be very discomforting. In the Y-direction, severe discomfort is observed for all wind directions at a wind speed of 60 m/s, and for a wind direction of 0°, severe discomfort is observed for wind speeds exceeding 42.5 m/s. For wind speeds greater than 55.0 m/s, floor accelerations become intolerable for occupants, indicating the building's collapse or imminent collapse. Overall, torsion does not significantly affect the motion comfort ranges of acceleration. This observation is further supported by inter-story drift values.

4.1.2. Inter-story drift ratios

Fig. 15 shows the peak inter-story drift ratios of the building in X-

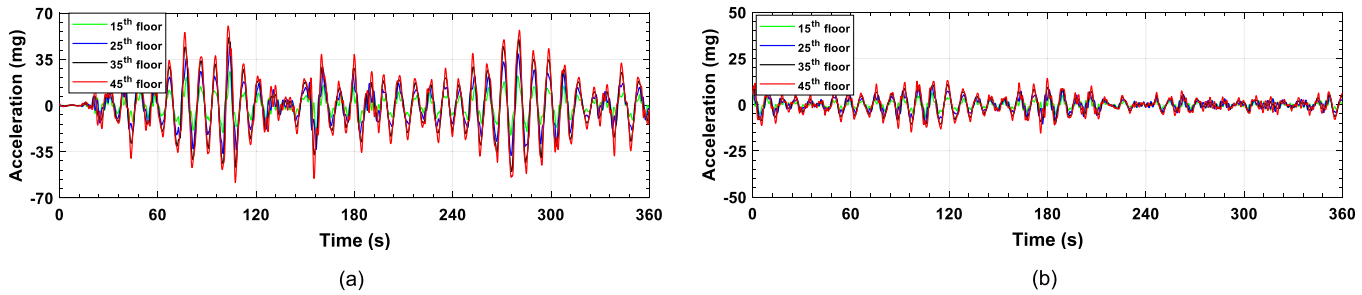

Fig. 10. Floor acceleration time histories of the building at wind speed of 40 m/s and wind direction of 90°: (a) X-direction, and (b) Y-direction.

and Y-directions as a function of wind velocity. The peak drift ratios are plotted for 10 wind directions between 0° and 90° (with an interval of 10°). As the building is flexible, the relatively large drift values are observed in both X-and Y-direction. Along with the drift value for various wind speeds and wind directions, the threshold limits corresponding to operational and continued occupancy performance levels are also plotted. Clearly, the drift values in X-direction exceed the upper limit for the operational performance level even at a wind speed of 25.0 m/s. As the wind speed is further increased, the drift increases significantly ultimately exceeding the upper limit of drift for continued occupancy with limited interruption performance level. Compared to the X-direction, relatively lower drift values are observed in the Y-direction. This investigation reveals that the wind direction governs the response of the buildings. The collapse of building happens with large story drifts in the X-direction, which happens when the wind speed is increased to 55.0 m/s and above. In particular, the building collapse is found to occur for the wind directions between 0° and 50°, which is remarked by significantly high value inter-story drifts. It should be noted that drift values above 0.40 are also observed for some cases.

4.1.3. Deformation damage index

Further, another performance criteria is evaluated which is related with performance of the cladding system due to large inter-story shear strain deformations. The DDI index in the X-direction and Y-direction are calculated using the displacements of two middle bays of the buildings on each two faces. Similar to the drift ratios, the DDI indices in the X-directions are significantly greater than in the Y-direction. Fig. 16 (b) shows the peak value of DDI indices measured in the X-directions of the building along with the shear deformation limits. The figure reveals that the exterior cladding panels of the building are expected to undergo significant damage for relatively moderate wind speeds. For wind speeds above 35.0 m/s, the DDI indices exceed the upper limit of 1/140. ASCE also suggests that the cladding should not fall from the building up to a DDI index of 0.02. In the case study, DDI indices are observed more than 0.02 in many cases. Therefore, it can be concluded that the building does not provide acceptable performance related to the serviceability design of cladding wall systems.

4.1.4. Demand to capacity index

Fig. 17 presents response of the building for wind direction of 0° and three different wind speeds, i.e., 50 m/s, 55 m/s, and 60 m/s. The figure shows the global response of the system using the relationship between base moment and roof drift ratio, and response of corner column using moment versus rotation relationship. Fig. 17(a) highlights the nonlinear relationship between the base moment and deformation of the system. The system failure coincides with the failure in the corner column, which is marked by large increase in drift/rotation. The responses of each structural member are calculated for the load combination defined in Equation 6. From the time history of axial, moment, and shear forces, the peak value of internal forces is obtained to calculate the DCIs. The DCIs are calculated for the interaction of axial forces, bending moment, and shear forces. In the analysis, the DCI values for shear are observed to be significantly low; therefore, they are not discussed in this study. Fig. 18 presents the response surface plot as a function of wind direction and wind speed for the corner perimeter column at first story of the building. As observed in the acceleration and drift values, the DCI indices are observed strongly dependent on the wind directions as well as wind speed. A DCI index of 1.0 implies that the demand on the structural member exceeds the capacity of the member. For wind direction between 10° and 50°, and wind speeds greater than 55.0 m/s, the DCI indices are observed greater than 1. For wind direction of 0°, the DCI values are observed to be 0.49 and 1.40 for the wind speed of 55.0 m/s and 60.0 m/s, respectively. A maximum value of 1.84 for DCI is observed for the wind direction of 20° and wind speed of 60.0 m/s.

For a detailed investigation, the DCI values for the columns at 1st, 16th, and 31st story are calculated. These stories are selected due to the change in cross-section dimensions of columns at these stories. In the next step, Fig. 19 shows the DCI values of the core columns at three stories for different wind directions and wind speeds. For the wind speed of 25.0 m/s, the DCI values are observed as low as 0.10. These DCI values for the core columns increase significantly with the increase in wind speed. Along with the increase in DCI values, the distribution of DCI values is also observed to be more dispersed for higher wind speeds. For wind speed of 60.0 m/s, the DCI values of the first story columns are observed in the range between 0.5 and 1.8. In the first story columns, a considerable number of core columns can be found to have DCI values greater than 1.0. Similar observations can be made from the DCI values

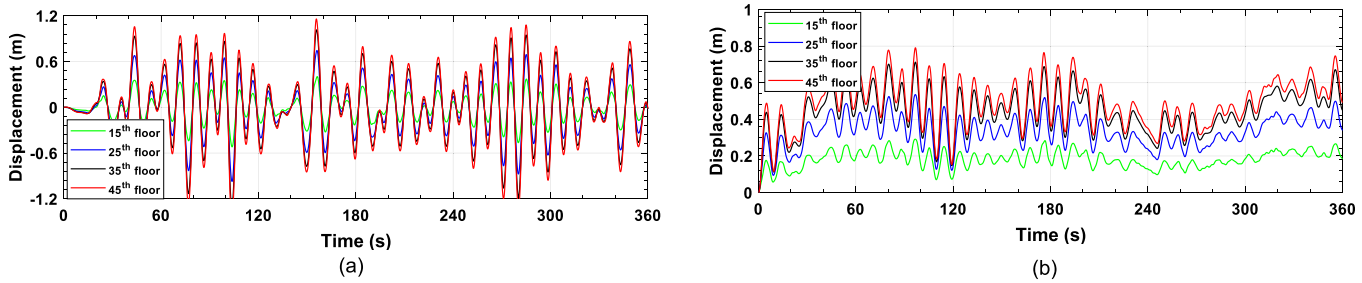

Fig. 11. Floor displacement time histories of the building at wind speed of 40 m/s and wind direction of 90°: (a) X-direction, and (b) Y-direction.

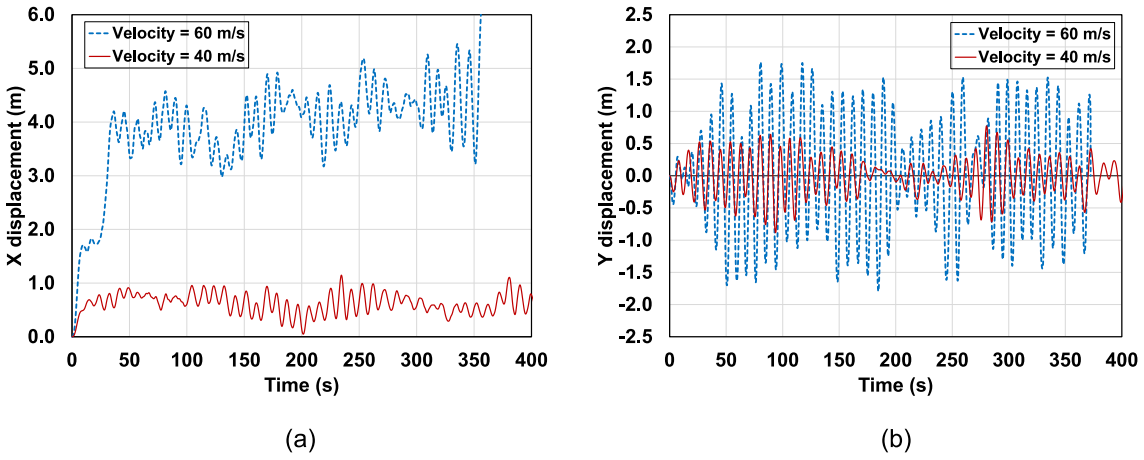

Fig. 12. Top floor displacement time histories of the building at wind speed of 40 and 60 m/s and wind direction of 0°: (a) X-direction, and (b) Y-direction.

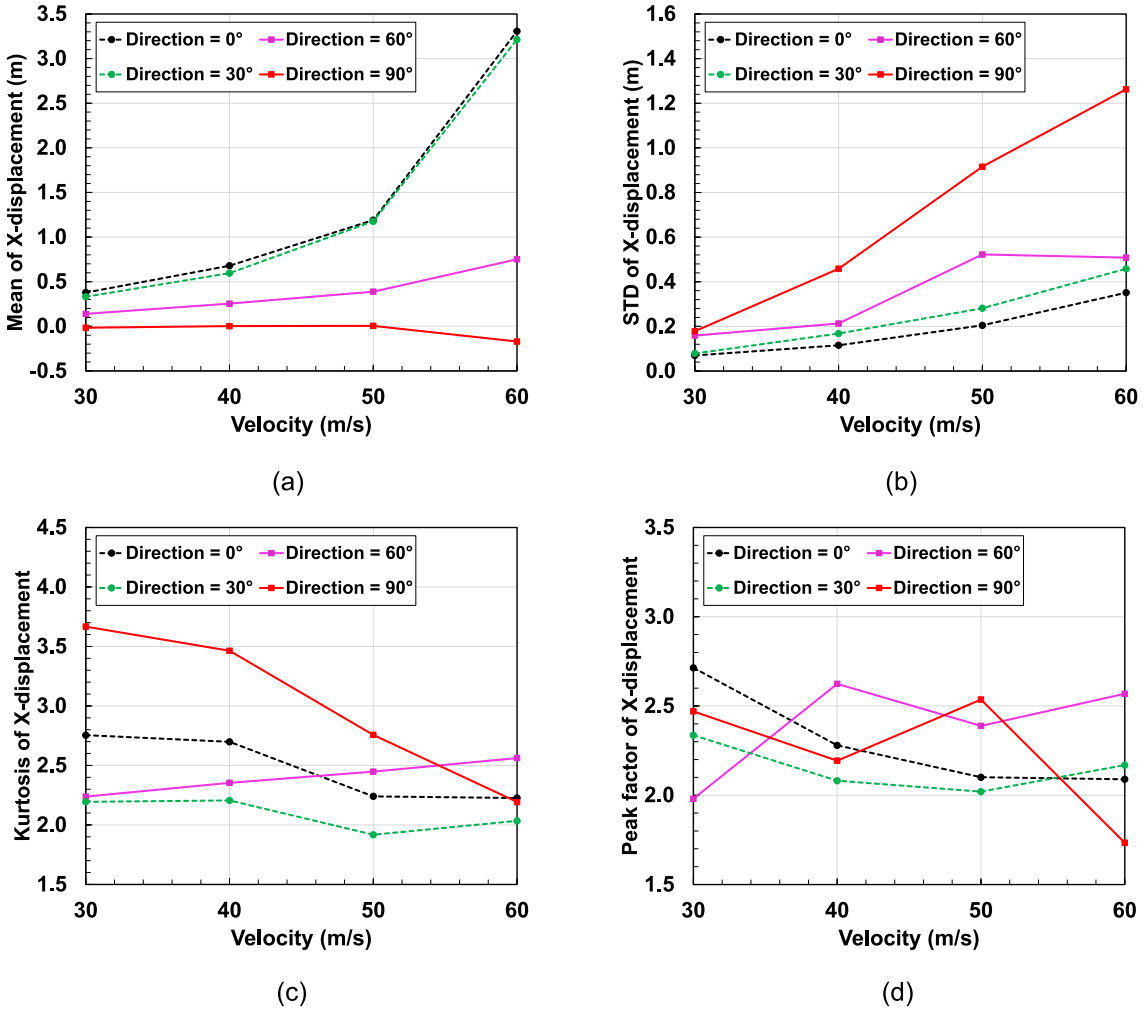

Fig. 13. Statistical moments for top floor X-direction displacement: (a) Mean, (b) Standard deviation, (c) Kurtosis, (d) Peak factor.

of core columns at 16th floor as shown in Fig. 19(b). As compared to columns at 1st floor, these columns are found to be less stressed as indicated by the highest DCI value of 1.38. Fig. 19(c) presents the DCI values for the core columns at 31st floor. As expected for columns on higher floors, even for the wind speed of 60.0 m/s, the wind-induced demand does not exceed the capacity in any of the core columns at 31st floor. From Fig. 19(d), a maximum DCI value of 0.87 can be observed for the wind speed of 60.0 m/s.

In the next step, the DCI indices of the perimeter columns are investigated. Fig. 20 presents the DCI indices of the perimeter columns at three stories for different wind directions and wind speeds. As compared to core columns, the perimeter columns are slightly more stressed due to the smaller cross-section and increased moments. For the wind speed of 60.0 m/s, the DCI indices for the perimeter columns at 1st

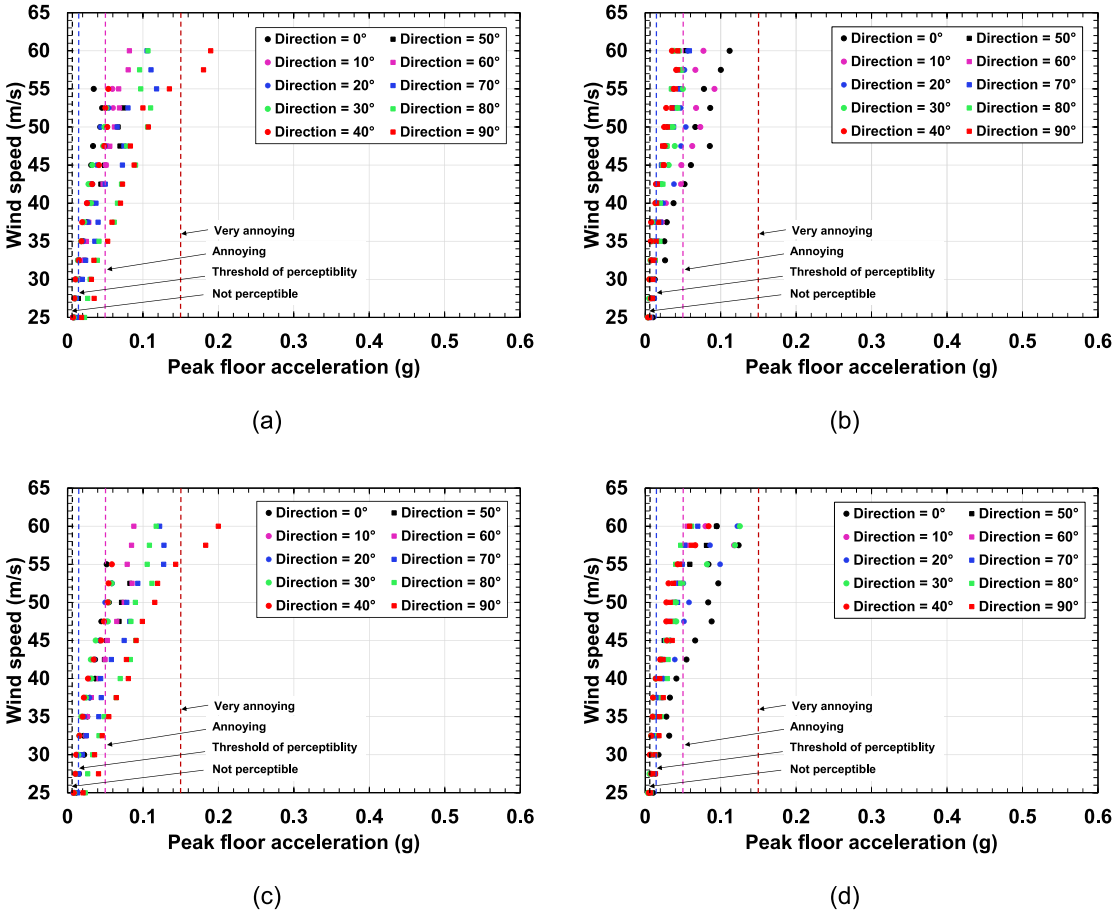

Fig. 14. Performance evaluation of the building subjected to occupant comfort level: (a) floor's center acceleration in X-direction, and (b) floor's center acceleration in Y-direction, (c) floor's corner acceleration in X-direction, and (d) floor's corner acceleration in Y-direction..

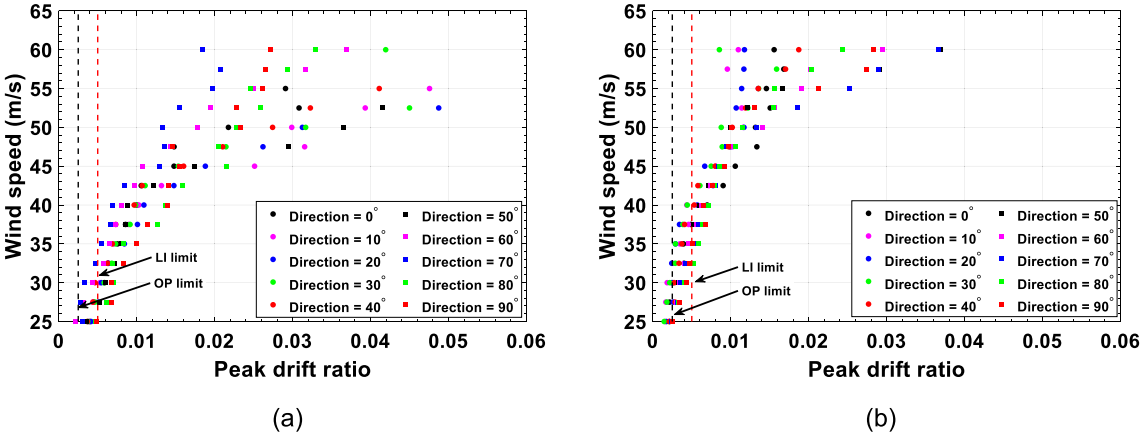

Fig. 15. Inter-story drift ratios of the building as a function of wind speed: (a) inter-story drift ratios in X-direction, and (b) inter-story drift ratios in Y-direction.

story ranges between 0.6 and 2.0. As observed in the core columns, a considerable number of perimeter columns are observed to exceed their capacity for wind speeds greater than 55.0 m/s. Fig. 20(b) shows the DCI indices for the perimeter columns at 16th story. As expected, these columns are less stressed as compared to perimeter columns at 1st story. This can be identified from the fact that most of the perimeter columns have a DCI index less than 0.30 for wind speeds between 25.0 m/s and 60.0 m/s. However, some of the perimeter columns at 16th story are observed to have DCI index greater than 1.0 with a maximum value of 1.42. To extend this investigation, the DCI index of perimeter columns at 31st story is calculated which are show in Fig. 20(c). From Fig. 20(c), none of the columns have a DCI index of greater than 1.0. However, a larger scatter in DCI indices is observed for wind speeds greater than 55.0 m/s. between the different angles of attack. This implies that the structural response of the columns varies significantly with wind direction.

The investigation revealed how the combination of wind direction and wind speed can influence the response of the building. This gives

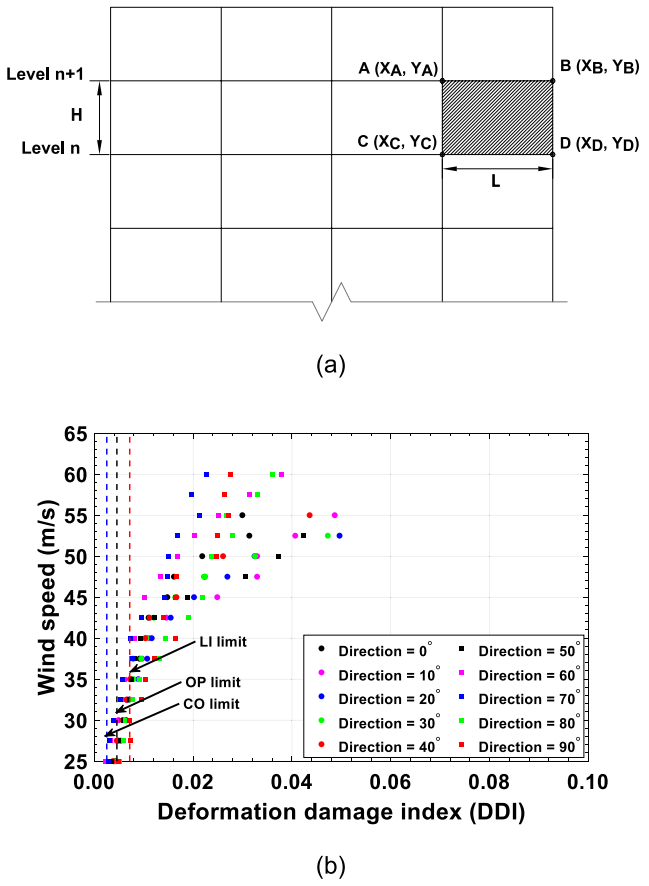

Fig. 16. (a) Calculation of damage deformation index (DDI), and (b) DDI indices in the X-direction.

insight into the design problem, which can significantly influence the performance of building. It is also revealed that analysis with only a fixed number of wind direction cannot provide the worst-case scenarios for the structural responses. Therefore, the actual performance of the building is determined after applying the wind directionality effects.

4.2. Peak directional response based on local climate data

In this study, climatological database consisting of wind speed data of 999 simulated hurricanes with 16 wind directions is considered. The

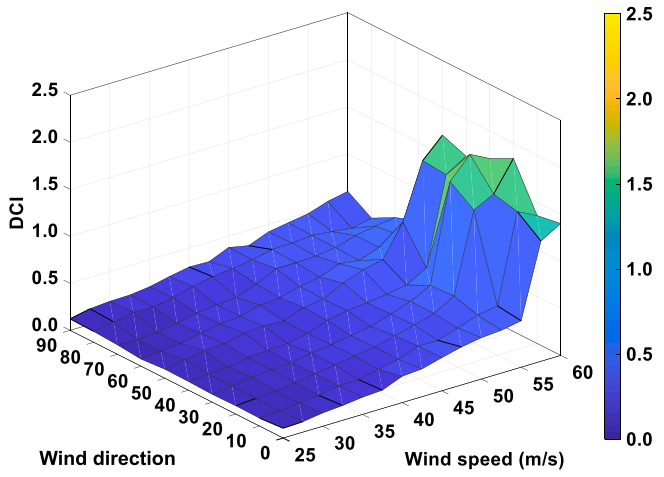

Fig. 18. Response surface plot for the DCI index of corner column at first floor.

climatological database is for a location near Newark, NJ (Milepost 2500), which is obtained from NIST (www.nist.gov/wind). The data set consists of simulated 1-minute hurricane wind speeds (in knots) at 10 m above ground. Using the procedure defined in Park and Yeo [34], the wind speed data is converted into mean hourly wind speeds at 10 m height. The building is assumed to be suburban terrain from all directions. The decay in hurricane intensity is not considered in this study. Fig. 21 shows the wind rose diagram for the 16 wind directions of the two climatological databases i.e., 22.5° to 360° (at an interval of 22.5°). From the figure, the direction of the extreme wind speeds is observed to be in the north direction. From the response surfaces, the directional responses for acceleration, inter-story drift ratio, and the DCI values are obtained using the procedure defined in Section 2.1. The directional responses of the wind effects are plotted as a function of MRIs. Fig. 22 shows the extreme response of acceleration (RMS value) and peak drift values as a function of MRI along with the various performance levels. The serviceability performance corresponding to occupant comfort is determined using the acceleration limits as prescribed by Chang [38] and ISO 10137 [39]. For this performance level, the acceleration values are checked for 10-year MRI. After applying the wind directionality effects, a peak acceleration value of 0.010 g is obtained which is in the range of threshold of perceptibility, according to Table 3. On the other hand, ISO 10137 [39] utilizes Fig. 1 to calculate the acceptance criteria. For residential buildings, ISO 10137 [39] provides a limiting value of 0.0064 g for 10 years MRI. Thus, the building satisfies the serviceability

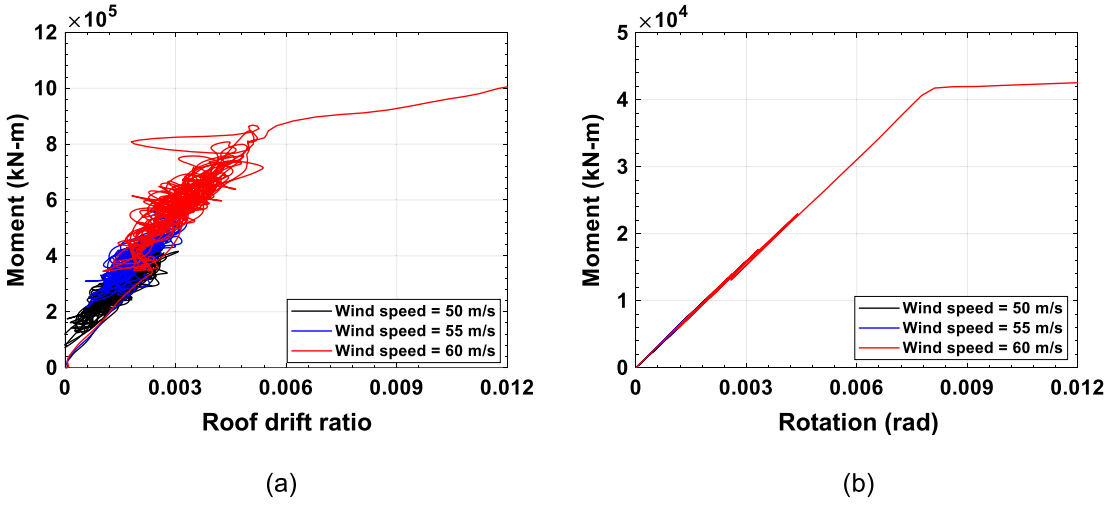

Fig. 17. Response of the building at different wind speeds: (a) global response, and (b) moment-rotation of the corner column at ground floor.

design criteria related to occupant comfort according to Chang [38] but does not provide acceptable performance according to ISO 10137 [39].

Now, serviceability requirement corresponding to inter-story drifts is evaluated. For the operational limit state, three MRIs of 10 years, 25 years, and 50 years are defined for three risk categories. On the other hand, the performance level of continuous occupancy with limited interruption must be checked for 700 years, 1700 years, and 3000 years corresponding to three risk categories. Fig. 22(b) shows the peak drift ratios in the X- and Y-direction as a function of MRI. For comparison, the upper limits of drift ratio corresponding to the two performance levels are also plotted. As seen in the figure, the response of the building in the two orthogonal directions exceeds the limit states for all MRIs. Further, the peak deformation damage index is calculated in the two directions and compared with limits. For comparison purposes, it is assumed that the building has metal claddings. For the operational limit state, the DDI limit is 0.01, whereas a value of 0.02 is considered for the performance level of continuous occupancy with limited interruption. Fig. 23 shows the peak DDIs in the X- and Y-direction as a function of MRI. The cladding along the Y-direction is observed to satisfy the performance thresholds but fails to satisfy the requirements in the X-direction. From the performance assessment corresponding to inter-story drifts and damage deformation index, the building does not provide acceptable performance in the two directions. Thus, it is essential to stiffen the building to achieve the desired objectives according to the performance-based design framework proposed in this paper.

In addition to the serviceability requirements, performance of the building is evaluated by checking strength design of the building. This is done by checking the DCI indices of the structural members at different MRIs. Fig. 24 shows DCI indices of the core columns and perimeter columns at 1st story as a function of MRI. For comparison, the limiting values of the DCI index for different performance levels are also plotted. As compared to the core columns, the perimeter columns are observed to show a wider distribution of DCI indices at a particular MRI. It is clear from the figure that both the core columns and perimeters satisfy the strength design requirements corresponding to occupant comfort and operational limit state. The DCI values are always found to below 1.0 up to 450 years MRI. For the third limit state, the DCI indices are only observed to satisfy the criteria for Risk category II. For Risk category III and IV, the DCI indices for the core columns and perimeters exceed the limited requirement of the Continuous occupancy, limited interruption performance level.

The structural system was designed following ASCE 7–16 such that the demand to capacity ratio of the structural members does not exceed one for a mean wind speed of 105.0 mph (46.9 m/s). According to ASCE 7–16, the 3-second gust wind speed specified for Newark city, considering exposure category C and Risk Category II, is 115 mph (51 m/s) at a height of 33 ft (10 m) above the ground. However, when considering the logarithmic wind profile law [46], the 3-second gust wind speed for the specific height of the building and its urban exposure is calculated to be 160 mph (71.5 m/s). From the simulations, it is observed that the system will experience collapse for a wind speed of 134.2 mph (60.0 m/s). This shows that the system can continue to withstand wind load based on mean hourly wind speed, when the structural members are in post-elastic range. From the perspective of strength design, the building satisfies the requirements for the occupant comfort and operational performance levels, while it also satisfies the continuous occupancy, limited interruption in Risk category II. Considering the 3-second gust wind speed of 160 mph (71.5 m/s), it becomes evident that the structure experiences capacity limitations within its inelastic range. While the building can withstand wind loads at the mean hourly wind speed, it demonstrates reduced capacity when subjected to extreme gusts. The performance assessment of the building reveals that the building fails to

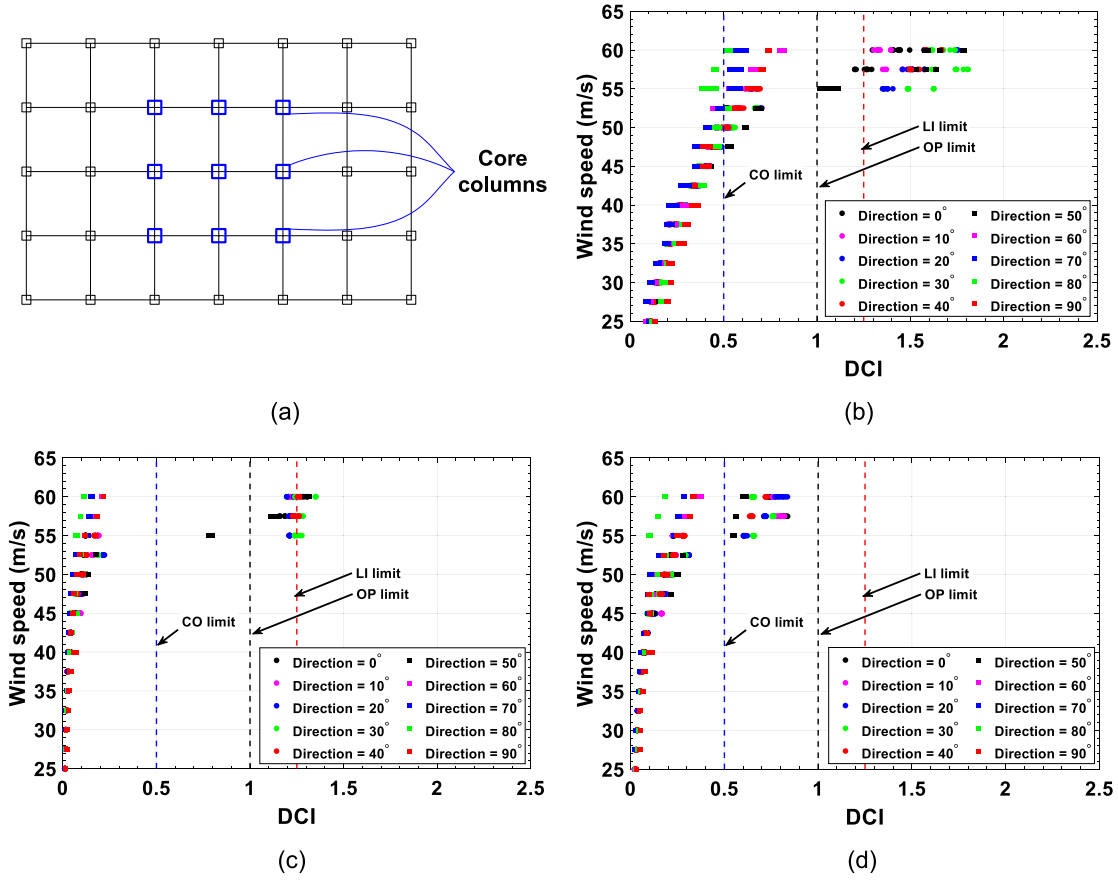

Fig. 19. DCI index for core columns as a function of wind speeds for the columns at: (a) structure plan, (b) 1st story, (c) 16th story, and (d) 31st story.

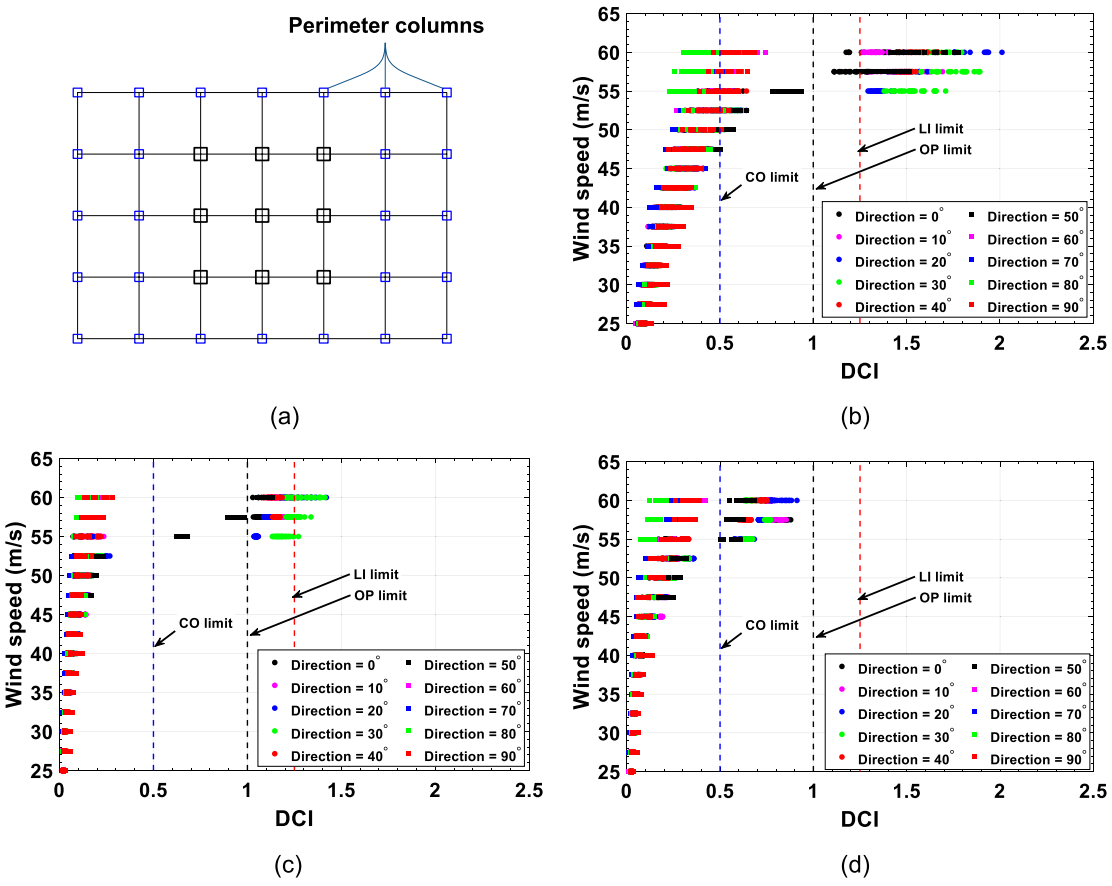

Fig. 20. DCI index for perimeter columns as a function of wind speeds for the columns at: (a) structure plan, (b) 1st story, (c) 16th story, and (d) 31st story.

satisfy the serviceability requirement of drifts. This is primarily due to flexibility of the building, which can be addressed by revising the design of building using bracings or dampers.

5. Summary and discussions

This paper investigates the performance of a tall steel building in time domain following the PBWD approach. The performance objectives and the acceptance criteria are defined, which are typically used for

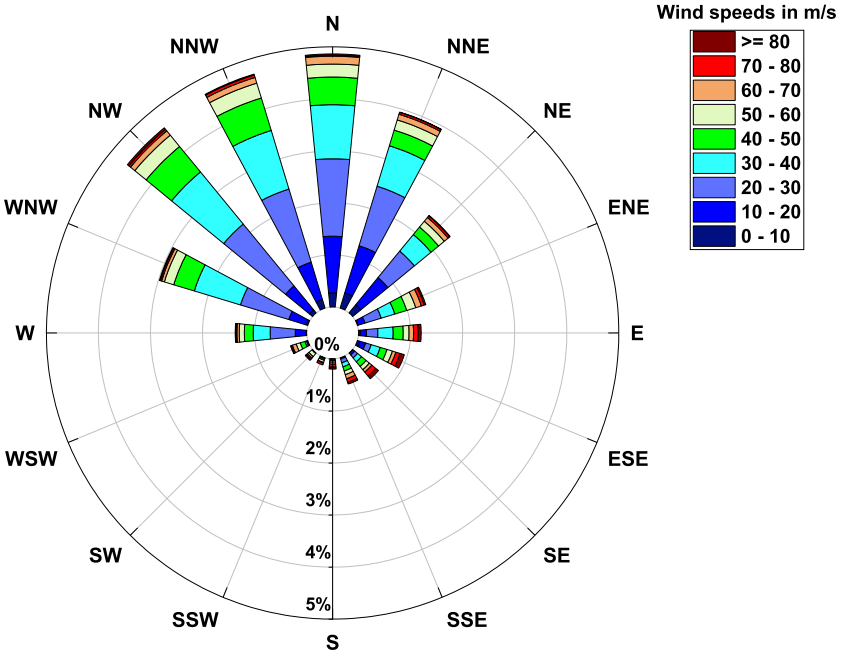

Fig. 21. Mean hourly wind rose diagram at 10 m height for the local climatological data in Newark, NJ (Milepost 2500).

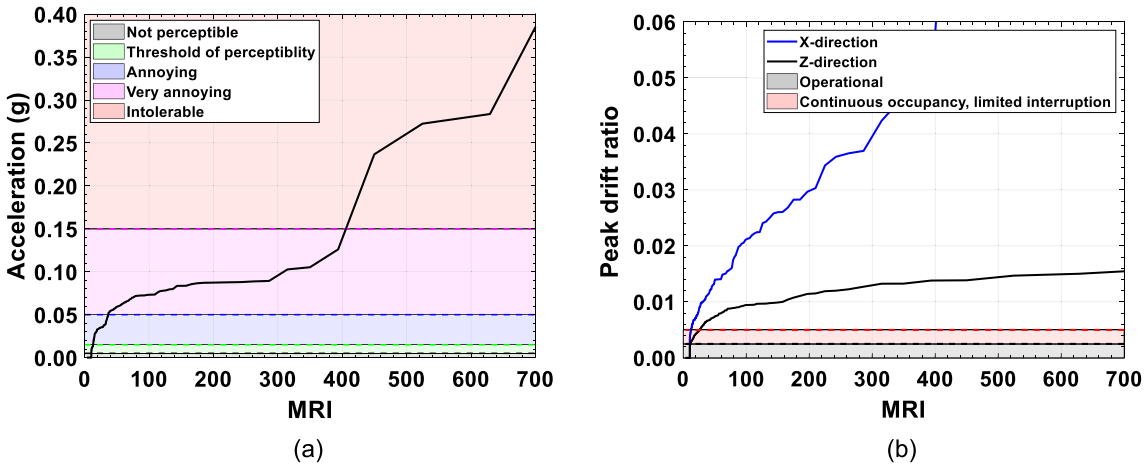

Fig. 22. Peak wind effects as a function of MRIs related to serviceability design: (a) Peak floor acceleration, and (b) inter-story drift ratios.

performance-based wind design. Three performance levels are defined i.e., occupant comfort, operational, and continued occupancy with limited interruption. To illustrate the proposed approach, a 45-story tall steel moment resisting frame building is selected for the case study. In this study, a nonlinear time history analysis is used to evaluate the response of the building subjected to wind loads of 30 min duration. The aerodynamic wind loads are obtained from the time histories of pressure coefficients measured in wind tunnel laboratory. A comprehensive analysis is performed for wind directions between 0° and 90°, and wind speed ranging from 25.0 m/s to 60.0 m/s. For each analysis, the key response measures such as acceleration, inter-story drift ratios, DDIs and DCIs are obtained to get the response surfaces. The performance of the building is evaluated after evaluating the directional response of the building. For that purpose, the climatological database of local building site is used. The main highlights of this study are as follows:

- The proposed framework provides the most accurate estimation of wind effects reflecting the variability of local wind climate. Since proposed PBWD is a direct simulation approach, the wind effects are obtained as a function of MRIs, which can be compared with different performance levels.
- In the case study, the structural system was designed following ASCE 7-16 such that the demand to capacity ratio of the structural members do not exceed 1 for a mean wind speed of 105.0 mph (46.9 m/s). The simulation result showed that the system may experience collapse for a wind speed of 134.2 mph (60.0 m/s). This shows that the building was able to withstand the wind loads for wind speeds 1.27 times the ASCE 7–16 prescribed values. The inclusion of controlled nonlinear response of the building may result in economic and efficient structural designs. A controlled inelastic behavior can reduce structural damage and prevent structural collapse.
- The performance related to serviceability design of the building is evaluated by using three different criteria i.e., floor accelerations, inter-story drifts, and DDI. The peak accelerations of the buildings are observed to be at the roof level, while the peak story drifts are observed to be maximum at 15th and 16th story during the linear response of building. In the nonlinear range, the peak drifts are observed at the 44th and 45th floor. Due to the high flexibility of the building, accelerations and story drifts are observed to be significantly higher along the minor axis of the building.
- From the response surfaces of inter-story drift ratios, the across wind response is found to be more dominant than the along wind responses for several wind directions. Without incorporating the wind directionality effects, the story drift ratios exceed the performance criteria of the three performance levels, even at moderately low wind speeds. The shear deformation of the exterior wall cladding is evaluated using the DDI. For the investigated wind directions and wind speeds, the DDI is observed to be greater than 0.02 for several wind directions when wind speed is more than 45 m/s, implying unacceptable performance of the cladding wall systems.
- From the response surfaces of DCIs, it is found that DCI values are not proportional to the square of wind speed. The DCI values are found to depend on wind directions and interactions between the wind flow and the structure. With the increase in wind speed, the scatter in the DCI indices increase for both core columns and perimeters. On comparing, the DCI indices of perimeter columns are observed to be slightly higher than the perimeter columns. Overall, the DCI indices are observed to be maximum for the columns at 1st floor.
- The performance of the building for different performance levels is evaluated after incorporating the wind directionality effects. For the occupant comfort, the acceleration are found to be within limits according to Chang [38] but fails to satisfy the criteria in ISO [39]. The building fails to satisfy the serviceability requirement of drifts at all performance levels. This is primarily due to flexibility of the building. From the perspective of strength design, the building satisfies the requirements for the occupant comfort and operational performance levels, while it also satisfies the continuous occupancy, limited interruption in Risk category II.

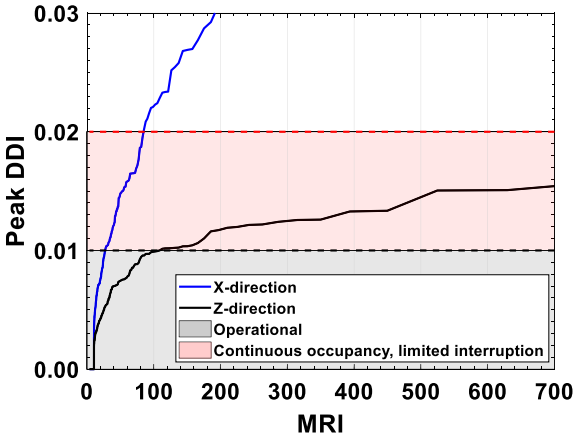

Fig. 23. Peak damage deformation index as a function of MRIs related to serviceability design.

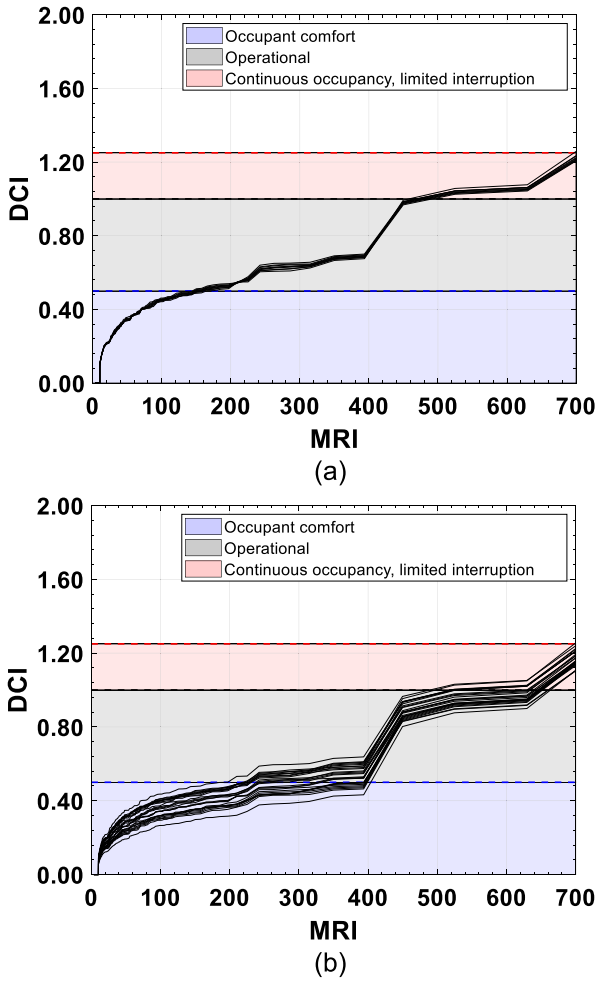

Fig. 24. Peak DCI indices as a function of MRIs for columns at 1st story: (a) core columns, and (b) perimeter columns.

CRediT authorship contribution statement

Dikshant Saini: Data curation, Formal analysis, Investigation, Methodology, Software, Validation, Visualization, Writing – original draft. **Bahareh Dokhaei:** Data curation, Software. **Behrouz Shafei:** Supervision, Writing – review & editing. **Alice Alipour:** Conceptualization, Funding acquisition, Investigation, Methodology, Project administration, Resources, Supervision, Validation, Writing – review & editing.

Declaration of competing interest

The authors declare that they have no known competing financial interests or personal relationships that could have appeared to influence the work reported in this paper.

Data availability

Data will be made available on request.

Acknowledgments

This paper is based upon work supported by the National Science Foundation under Grants No. 2214039 and 1826356. This support is gratefully acknowledged. Any opinions, findings, and conclusions or recommendations expressed in this material are those of the authors and do not necessarily reflect the views of the sponsor.

References

[1] Emanuel K. Increasing destructiveness of tropical cyclones over the past 30 years. Nature 2005;436(7051):686–8. Nature Publishing Group.
[2] Karl TR, Melillo JM, Peterson TC, Hassol SJ. Global climate change impacts in the United States. Cambridge University Press; 2009.
[3] Mendelsohn R, Emanuel K, Chonabayashi S, Bakkensen L. The impact of climate change on global tropical cyclone damage. Nat Clim Chang 2012;2(3):205–9. Nature Publishing Group.
[4] Abdelaziz KM, Alipour A, Hobeck JD. A smart façade system controller for optimized wind-induced vibration mitigation in tall buildings. J Wind Eng Ind Aerodyn 2021;212. https://doi.org/10.1016/j.jweia.2021.104601.
[5] Hareendran SP, Alipour A, Sarkar P. Improving aerodynamic response of tall buildings using smart morphing facades. J Build Eng 2023;80. Elsevier.
[6] Hou F, Sarkar PP, Alipour A. A novel mechanism – smart morphing façade system - to mitigate wind-induced vibration of tall buildings. Eng Struct 2023;275. https://doi.org/10.1016/j.engstruct.2022.115152.
[7] Jafari M, Alipour A. Methodologies to mitigate wind-induced vibration of tall buildings: A state-of-the-art review. J. Build Eng 2021.
[8] Jafari M, Alipour A. Aerodynamic shape optimization of rectangular and elliptical double-skin façades to mitigate wind-induced effects on tall buildings. J Wind Eng Ind Aerodyn 2021;213. https://doi.org/10.1016/j.jweia.2021.104586.
[9] Saini D, Alipour A, Heckert NA, Simiu E. Design of high-rise buildings with arbitrary shapes for multi-directional wind. Structures 2023. 105007, Elsevier.
[10] Pre-standard ASCE. Prestandard for performance-based wind design. American Society of Civil Engineers; 2019.
[11] Bartoli G, Ricciardelli F, Saetta A, Sepe V. Performance of wind exposed structures. results of the PERBACCO project. Firenze University Press; 2006.
[12] Ciampoli M, Petrini F, Augusti G. Performance-based wind engineering: towards a general procedure. Struct Saf 2011;33(6):367–78. Elsevier.
[13] Griffis L, Patel V, Muthukumar S, Baldava S. A framework for performance-based wind engineering. In: Advances in hurricane engineering: Learning from our past; 2013. p. 1205–16.
[14] Petrini F. A probabilistic approach to performance-based wind engineering (PBWE); 2009.
[15] Solari G. Wind-excited response of structures with uncertain parameters. Probab Eng Mech 1997;12(2):75–87. Elsevier.
[16] Hart GC, Jain A. Performance-based wind evaluation and strengthening of existing tall concrete buildings in the Los Angeles region: dampers, nonlinear time history analysis and structural reliability. Struct Design Tall Spec Build 2014;23(16):1256–74. Wiley Online Library.
[17] Judd JP, Charney FA. Inelastic behavior and collapse risk for buildings subjected to wind loads. Structures Congress 2015;2015:2483–96.
[18] Li Y-Q, Tamura Y. Nonlinear dynamic analysis for large-span single-layer reticulated shells subjected to wind loading. Wind Struct 2005;8(1):35–48. Techno-Press.
[19] Micheli L, Alipour A, Laflamme S. Multiple-surrogate models for probabilistic performance assessment of wind-excited tall buildings under uncertainties. ASCE ASME J Risk Uncertain Eng Syst A Civ Eng 2020;6(4):04020042. American Society of Civil Engineers.
[20] Mohammadi A, Azizinamini A, Griffis L, Irwin P. Performance assessment of an existing 47-story high-rise building under extreme wind loads. J Struct Eng 2019;145(1):4018232. American Society of Civil Engineers.
[21] Muthukumar S, Baldava S, Garber J. Performance-based evaluation of an existing building subjected to wind forces. In: Advances in hurricane engineering: Learning from our past; 2013. p. 1217–28.
[22] Solari G, Piccardo G. Probabilistic 3-D turbulence modeling for gust buffeting of structures. Probab Eng Mech 2001;16(1):73–86. Elsevier.
[23] Ghaffary A, Moustafa MA. Performance-Based Assessment and Structural Response of 20-Story SAC Building under Wind Hazards through Collapse. J Struct Eng 2021;147(3):4020346. American Society of Civil Engineers.
[24] Chuang W-C, Spence SMJ. An efficient framework for the inelastic performance assessment of structural systems subject to stochastic wind loads. Eng Struct 2019;179:92–105. Elsevier.
[25] Ouyang Z, Spence SMJ. A performance-based wind engineering framework for envelope systems of engineered buildings subject to directional wind and rain hazards. J Struct Eng 2020;146(5):4020049. American Society of Civil Engineers.
[26] Hareendran SP, Alipour A. Prediction of nonlinear structural response under wind loads using deep learning techniques. Appl Soft Comput 2022;129. Elsevier.
[27] Hareendran SP, Alipour A, Shafei B, Sarkar P. Characterizing wind-structure interaction for performance-based wind design of tall buildings. Eng Struct 2023;289. Elsevier.
[28] Jeong SY, Alinejad H, Kang TH-K. Performance-based wind design of high-rise buildings using generated time-history wind loads. J Struct Eng 2021;147(9):04021134. American Society of Civil Engineers.
[29] Huang J, Chen X. Inelastic performance of high-rise buildings to simultaneous actions of alongwind and crosswind loads. J Struct Eng 2022;148(2). 04021258, American Society of Civil Engineers.
[30] Feng C, Chen X. Inelastic responses of wind-excited tall buildings: Improved estimation and understanding by statistical linearization approaches. Eng Struct 2018;159:141–54. Elsevier.
[31] Huang J, Chen X. Inelastic response of high-rise buildings under strong winds: accuracy of reduced-order building model and influence of biaxial response interaction. J Struct Eng 2023;149(1). 04022211, American Society of Civil Engineers.

[32] Abdelwahab M, Ghazal T, Nadeem K, Aboshosha H, Elshaer A. Performance-based wind design for tall buildings: Review and comparative study. J Build Eng 2023. 106103, Elsevier.
[33] Preetha Hareendran S, Alipour A, Shafei B, Sarkar P. Performance-based wind design of tall buildings considering the nonlinearity in building response. J Struct Eng 2022;148(9):04022119. American Society of Civil Engineers.
[34] Park S, Yeo D. Database-assisted Design and Equivalent Static Wind Loads for Mid- and High-rise Structures: Concepts, Software, and User's Manual. US Department of Commerce, National Institute of Standards and Technology; 2018.
[35] Rigato A, Chang P, Simiu E. Database-assisted design, standardization, and wind direction effects. J Struct Eng 2001;127(8):855–60. American Society of Civil Engineers.
[36] Whalen TM, Sadek F, Simiu E. Database-assisted design for wind: basic concepts and software development. J Wind Eng Ind Aerodyn 2002;90(11):1349–68. Elsevier.
[37] ASCE 7-16. 2016. Minimum Design Loads and Associated Criteria for Buildings and Other Structures. ASCE/SEI 7-16.
[38] Chang F-K. Human response to motions in tall buildings. J Struct Div 1973;99(6): 1259–72. American Society of Civil Engineers.
[39] International Organization for Standardization. Bases for design of structures-serviceability of buildings and walkways against vibration. International Standard, ISO; 2007. p. 10137.
[40] Boggs D, Lepage A. Wind tunnel methods. Special Publication 2006;240:125–42.
[41] Garber J, Browne MTL, Xie J, Kumar KS. Benefits of the pressure integration technique in the design of tall buildings for wind. ICWE12 Cairns; 2007.
[42] Ho TC, Jeong UY, Case P. Components of wind-tunnel analysis using force balance test data. Wind Struct 2014;18(4):347–73. Techno-Press.
[43] Huang G, Chen X. Wind load effects and equivalent static wind loads of tall buildings based on synchronous pressure measurements. Eng Struct 2007;29(10): 2641–53. Elsevier.
[44] AISC 360-16. 2016. AISC 360-16-Specification for Structural Steel Buildings. Chicago AISC.
[45] Griffis LG. Serviceability limit states under wind load. Eng J 1993;30(1):1–16.
[46] Simiu E, Yeo D. Wind effects on structures: modern structural design for wind. John Wiley & Sons; 2019.
[47] Carta JA, Ramirez P, Bueno C. A joint probability density function of wind speed and direction for wind energy analysis. Energy Convers Manag 2008;49(6): 1309–20. Elsevier.
[48] PEER (Pacific Earthquake Engineering Research). OpenSees: A Framework for Earthquake Engineering Simulation (OpenSEES). Berkeley, CA: University of California, IEEE; 2015.
[49] Lignos DG, Krawinkler H. Deterioration modeling of steel components in support of collapse prediction of steel moment frames under earthquake loading. J Struct Eng 2011;137(11):1291–302. American Society of Civil Engineers.
[50] Gupta A, Krawinkler H. Estimation of seismic drift demands for frame structures. Earthq Eng Struct Dyn 2000;29(9):1287–305. Wiley Online Library.
[51] Yamada S, Suita K, Tada M, Kasai K, Matsuoka Y, Shimada Y. Collapse experiment on 4-story steel moment frame: Part 1 outline of test results. Proceedings of the 14th world conference on earthquake engineering, Beijing, China; 2008.
[52] Lignos DG, Hikino T, Matsuoka Y, Nakashima M. Collapse assessment of steel moment frames based on E-Defense full-scale shake table collapse tests. J Struct Eng 2013;139(1):120–32.
[53] Ding J, Chen X. Assessment of methods for extreme value analysis of non-Gaussian wind effects with short-term time history samples. Eng Struct 2014;80:75–88. Elsevier.